

Learning to Initialize Gradient Descent Using Gradient Descent

Kartik Ahuja*

Amit Dhurandhar*

Kush R. Varshney*

Abstract

Non-convex optimization problems are challenging to solve; the success and computational expense of a gradient descent algorithm or variant depend heavily on the initialization strategy. Often, either random initialization is used or initialization rules are carefully designed by exploiting the nature of the problem class. As a simple alternative to hand-crafted initialization rules, we propose an approach for learning “good” initialization rules from previous solutions. We provide theoretical guarantees that establish conditions that are sufficient in all cases and also necessary in some under which our approach performs better than random initialization. We apply our methodology to various non-convex problems such as generating adversarial examples, generating post hoc explanations for black-box machine learning models, and allocating communication spectrum, and show consistent gains over other initialization techniques.

1 Introduction

In many machine learning and engineering tasks, we are often required to solve optimization problems repeatedly. For instance, a system that generates explanations for black-box machine learning models [Ribeiro et al., 2016] [Dhurandhar et al., 2018] needs to solve a new optimization problem for every new prediction made; a recommender system solves a different optimization problem [Koren et al., 2009, Mairal et al., 2010] every time a new subject arrives. Many of these optimization problems are non-convex, and initialization plays a crucial rule in finding a good local minimum. As is typically the case, the optimization problems for each instance are solved independently. However, if one were to learn “good” initializations for many of the instances based on previous solutions, it could lead to significant savings in time, money, and energy, where function and gradient evaluation has an associated cost and carbon footprint [Strubell et al., 2019]. In this work, we develop methods that *learn to initialize* based on past knowledge.

Over the recent years, several works, an incomplete representative list – [Andrychowicz et al., 2016] [Li and Malik, 2016] [Wichrowska et al., 2017] [Finn, 2018][Khalil et al., 2017] – have explored the “learning to optimize” paradigm. Departing from expert-driven design, these works study data-driven design of optimization algorithms for training machine learning models. They are inspired by the long line of work in meta-learning [Thrun and Pratt, 2012, Schmidhuber, 1987, Schmidhuber, 1992]. Gradient descent based algorithms [Nocedal and Wright, 2006] typically consist of two blocks: initialization and step updates (update direction, and learning rates). Works such as [Andrychowicz et al., 2016, Li and Malik, 2016, Wichrowska et al., 2017, Finn, 2018] primarily focus on learning step updates instead of following the standard step update rules. Many works such as [Antoniou et al., 2018,

*IBM Research, Thomas J. Watson Research Center, Yortown Heights, New York

Flennerhag et al., 2018, Finn et al., 2017] focus on learning good models that serve as good initialization for different few-shot learning tasks. In these works [Antoniou et al., 2018, Flennerhag et al., 2018, Finn et al., 2017], the parametrization/identity of the learning task is not known. Hence, these works adopt an approach that does not require a task’s identity as input to compute the initialization. However, in many optimization problems that are of interest to us (e.g., generating explanations and adversarial examples), we are given the identity of the optimization problem (e.g., prediction to be explained); we take advantage of this additional information herein.

Hand-designing initializers tailored to a specific problem class is common. For instance, in clustering [Arthur and Vassilvitskii, 2007, Pena et al., 1999], phase retrieval [Candes et al., 2015], and deep learning [Glorot and Bengio, 2010, Mishkin and Matas, 2015, Dauphin and Schoenholz, 2019], different elegant initialization rules have been proposed for the respective problem classes that work better than random initialization. However, it is impractical to develop these rules for every new optimization problem we encounter and a more scalable strategy is highly desirable. Hence, we aim to build a data-driven initialization approach that is scalable, adaptable, and learns initialization rules based on the identity of the optimization task.

We propose two methods. The first method uses objective function values whereas the second method uses argument values at the solution to learn the initializers. We establish mild conditions under which the methods are guaranteed to perform well and better than the random initialization. The first method is designed for non-convex problems, especially where the variance in local minimum values is large, and does not offer advantage in convex problems. The second method is designed to work in both convex and non-convex problems. We carry out extensive experiments to show that the proposed methods perform better than many of the existing approaches on several convex and non-convex optimization problems.

2 Problem formulation

We are given an objective function $f : \Theta \times \mathcal{X} \rightarrow \mathbb{R}$ to be minimized. The input to the function is divided in two categories:

- $\theta \in \Theta \subseteq \mathbb{R}^m$: the set of variables to be optimized,
- $x \in \mathcal{X} \subseteq \mathbb{R}^n$: the parameters that specify the identity of the optimization instance.

The minimization problem for instance x is given as

$$\min_{\theta \in \Theta} f(\theta, x), \tag{1}$$

For each $x \in \mathcal{X}$, the function $f(\cdot, x)$ is differentiable in θ for all θ in the interior of Θ . We use a gradient descent solver (see Algorithm 8), which we refer to as GD. GD takes as input an initialization θ_{in} and function $f(\cdot, x)$ corresponding to the instance x , and outputs the argument and function value at the solution. Define $g : \Theta \times \mathcal{X} \rightarrow \mathbb{R}$ to capture the relationship between the initialization θ_{in} , problem instance x , and the function value at the solution $g(\theta_{\text{in}}, x)$ found by GD. Similarly define g^\dagger , where $g^\dagger(\theta_{\text{in}}, x) \in \Theta$ is the argument value at the solution. If the number of iterations in GD is large and certain standard conditions are met (gradient of $f(\cdot, x)$ is Lipschitz continuous and step updates follow Wolfe conditions) [Nocedal and Wright, 2006], then GD converges to a *stationary point*. In such cases, g and g^\dagger are the function value and argument at the stationary point.

We are presented a sequence of instances $\{X_i\}_{i=1}^\infty$, drawn i.i.d. from a distribution \mathbb{P}_X . The sequence of functions corresponding to these instances are $\{f_i\}_{i=1}^\infty$, where $f_i = f(\cdot, X_i)$ is a function of θ for a fixed X_i . Our goal is to solve equation (1) repeatedly for $\{X_i\}_{i=1}^\infty$. Observe that we can use the information that we acquire from solving the optimization for past instances to improve the current search. We now provide motivating examples.

ML applications. Consider binary classification with labels in $\{1, -1\}$. Given a model $u : \mathbb{R}^m \rightarrow \mathbb{R}$, prediction $y = \text{sgn}(u(x))$. Consider the following problem:

$$\min_{\theta \in \Theta} \|\theta\|^2 + \beta \|\theta\|_1 \quad \text{s.t.} \quad y(u(x + \theta)) \leq 0. \quad (2)$$

If we set $\beta = 0$ and $\Theta = \mathbb{R}^m$, the problem is finding adversarial example for an instance x input to model u [Goodfellow et al., 2014]. θ is the smallest perturbation (attack) that moves x to the other side of the boundary $u(x) = 0$. If u is a deep neural network, then the above problem is non-convex and it is non-trivial to find the global optimum tractably. There is a lot of interest in understanding [Cheng et al., 2018, Cheng et al., 2019] whether an adversary can generate attacks with few queries to the model and its gradients. By exploiting the past adversarial instances, we show that the adversary can generate good adversarial examples with few queries.

If $\beta > 0$ and the set Θ is constrained to a special non-convex set referred to as ‘‘pertinent negatives’’ (PNs) [Dhurandhar et al., 2018], the problem in equation (2) is equivalent to finding instance-wise model explanations in the form of PNs. For a system that generates explanations on a repeated instance-to-instance basis (such as Fiddler AI, IBM Watson Openscale, H2O), it is important to generate these explanations fast and with a few model queries to minimize the user’s costs.

Engineering application. In a communication system [Chiang et al., 2007], users often transmit signals in the same spectrum and interfere with each other. Therefore, a base station must determine a spectrum sharing protocol. Consider a system with N senders and N receivers. Each sender i transmits at power level $\theta^i \in [0, 1]$. Define a channel matrix x , where the channel strength for sender i to the receiver j is $x[i, j] \in [0, 1]$. The rate at which sender i ’s data is transmitted to receiver i is given as $r_i(\theta, x) = \log(1 + \frac{x[i, i]\theta^i}{1 + \sum_{j \neq i} x[j, i]\theta^j})$, where $\theta = [\theta^1, \dots, \theta^N]$ is the power vector. The goal is to solve for $\theta \in [0, 1]^N$ maximizing $\sum_{i=1}^N r_i(\theta, x)$. This problem is referred to as ‘‘sum-rate optimization’’. In reality, the channel matrix x is not fixed and keeps changing [Tse and Viswanath, 2005]. As a result, the problem needs to be solved repeatedly thus making learning initialization important.

In all three examples described above, currently used optimization solvers repeatedly solve problem instances independently. Next, we describe how we can capture data from previous solves to improve future searches.

Scope of this work. Before proceeding, let us delineate problems which are not in the scope of current work, but could be fruitful avenues for future research. Our formulation is designed for scenarios in which individual task parametrization x values are known such as generating explanations, adversarial examples, etc. Consider we are training neural networks parametrized by $\theta \in \Theta$ for few-shot learning, i.e., finding networks that adapt quickly to a set prediction tasks $x \in \mathcal{X}$, where x characterizes the joint distribution of the features and the labels. In such cases, the objective defined in equation (1), $f(\theta, x)$, corresponds to the expected risk of model θ for task x . To apply our method to these tasks, x needs to be estimated, which is beyond the scope of current work. Model-agnostic meta-learning (MAML) [Finn et al., 2017] does not use x and thus is better suited for such few-shot learning tasks. We also do not focus on building initializers [Glorot and Bengio, 2010],

[Dauphin and Schoenholz, 2019] that specifically overcome the difficulties of training deep learning models.

Algorithm 1 Gradient Descent Algorithm (GD)

Input: function w , initial value θ_{in} , ϵ , iter_{max} , step size rules $\{t_k\}_{k=0}^{\infty}$, Π_{Θ} projection on the set Θ

Initialize: $\text{iter} = 0$

while $\text{iter} \leq \text{iter}_{\text{max}}$ and $\|\nabla_{\theta} w(\theta)\|_{\theta=\theta_{\text{iter}}} \geq \epsilon$ **do**

$\theta_{\text{iter}+1} = \Pi_{\Theta} \left[\theta_{\text{iter}} - t_{\text{iter}} \nabla_{\theta} w(\theta) \right]$

$\text{iter} = \text{iter} + 1$

end while

$\theta^{\dagger} = \theta_{\text{iter}}$, $w^{\dagger} = w(\theta_{\text{iter}})$

Output: θ^{\dagger} , w^{\dagger}

3 Learn to initialize gradient descent

3.1 Independent random vs. conditional random initialization

Define a random variable $\hat{\theta}$ with a distribution $\mathbb{P}_{\hat{\theta}}$ with support Θ . Independent random initialization method works as follows. For a problem instance X , GD is initialized using an independent draw of $\hat{\theta}$ and it finds a solution with objective value $\hat{Y} = g(X, \hat{\theta})$ (g was defined in Section 2). In this work, we develop a general form of initialization where the draw is conditioned on the problem instance $X \sim \mathbb{P}_X$. Define a random variable $\tilde{\theta}$ with a distribution $\mathbb{P}_{\tilde{\theta}|X}$. Conditional random initialization method works as follows. For a problem instance X , GD is initialized using a conditionally independent draw of $\tilde{\theta}|X$ and it finds a solution with objective value $\tilde{Y} = g(X, \tilde{\theta})$. The performance of standard random initialization is $\mathbb{E}_{X, \hat{\theta}}[\hat{Y}]$, while that of conditional random initialization is $\mathbb{E}_{X, \tilde{\theta}}[\tilde{Y}]$.

What are the minimum conditions on $\mathbb{P}_{\tilde{\theta}}$ to ensure that conditional random initialization $\tilde{\theta}$ is better than independent random initialization $\hat{\theta}$? The answer leads us to the principle underlying our main method. We carry out the analysis for a simple family of initializers $\tilde{\theta}$ that we define next. Consider two independent random initializations $\hat{\theta}_0 \sim \mathbb{P}_{\hat{\theta}}$ and $\hat{\theta}_1 \sim \mathbb{P}_{\hat{\theta}}$ with corresponding solution values $\hat{Y}_0 = g(X, \hat{\theta}_0)$ and $\hat{Y}_1 = g(X, \hat{\theta}_1)$ respectively. Define a random variable $Z \in \{0, 1\}$, where $Z|\hat{\theta}_0, \hat{\theta}_1, X$ is a Bernoulli random variable where $p(\hat{\theta}_0, \hat{\theta}_1, X)$ is the probability $Z = 0$. We define a family of initializers $\tilde{\theta}$ that select from one of the two initializers $\hat{\theta}_0, \hat{\theta}_1$ as $\tilde{\theta} = (1 - Z)\hat{\theta}_0 + Z\hat{\theta}_1$.

Assumption 1. (*Expected probabilistic ordering*) $\mathbb{E}_{X, \hat{\theta}_0, \hat{\theta}_1} \left[\left(p(\hat{\theta}_0, \hat{\theta}_1, X) - \frac{1}{2} \right) (\hat{Y}_0 - \hat{Y}_1) \right] < 0$.

If Assumption 1 holds, then for “some realizations” of $\hat{\theta}_0, \hat{\theta}_1$ and X , we know either $p(\hat{\theta}_0, \hat{\theta}_1, X) > \frac{1}{2}, \hat{Y}_0 < \hat{Y}_1$ or $p(\hat{\theta}_0, \hat{\theta}_1, X) < \frac{1}{2}, \hat{Y}_0 > \hat{Y}_1$. For such realizations, $\tilde{\theta}$ correctly orders the two initializations with probability more than $\frac{1}{2}$, which is just better than a random guess.

Proposition 1. (*Conditional vs. independent random*) Assumption 1 $\iff \mathbb{E}_{X, \tilde{\theta}}[\tilde{Y}] < \mathbb{E}_{X, \hat{\theta}}[\hat{Y}]$

The proofs to all the propositions are in the Appendix.

Remarks. Suppose GD converges to stationary points; in such a case $\tilde{\theta}$ described above compares stationary points. In addition, if $f(\cdot, x)$ is convex in θ for all $x \in \mathcal{X}$ and a minimizer exists in the

interior of Θ , then all the initializers are equally good as they reach the same global minimum value. As a result, Assumption 1 does not hold (since $\hat{Y}_0 = \hat{Y}_1$) and thus we cannot build a $\tilde{\theta}$ better than $\hat{\theta}$. Therefore, $\tilde{\theta}$ family described above is more suited for non-convex optimization problems.

Next, we consider a stricter version of Assumption 1 to understand the best possible performance achievable by initializers from the family $\tilde{\theta} = (1 - Z)\hat{\theta}_0 + Z\hat{\theta}_1$. We remove the expectation in Assumption 1 and require the probability of correct ordering to be larger than $\frac{1}{2}$.

Assumption 2. (*Probablistic ordering*) $\exists \gamma \in (\frac{1}{2}, 1]$
 $\hat{Y}_0 < \hat{Y}_1 \implies p(\hat{\theta}_0, \hat{\theta}_1, X) \geq \gamma, \hat{Y}_0 > \hat{Y}_1 \implies 1 - p(\hat{\theta}_0, \hat{\theta}_1, X) \geq \gamma.$

Proposition 2. (*Bounds on conditional random initialization*) Assumption 2 \implies

$$\mathbb{E}_{X, \hat{\theta}_0, \hat{\theta}_1}[\min\{\hat{Y}_0, \hat{Y}_1\}] \leq \mathbb{E}_{X, \tilde{\theta}}[\tilde{Y}] \leq \gamma \mathbb{E}_{X, \hat{\theta}_0, \hat{\theta}_1}[\min\{\hat{Y}_0, \hat{Y}_1\}] + (1 - \gamma) \mathbb{E}_{X, \hat{\theta}_0, \hat{\theta}_1}[\max\{\hat{Y}_0, \hat{Y}_1\}].$$

In non-convex optimization, many solvers used in practice follow a multi-start based approach, i.e., do multiple random initializations and then use the best solution [Hu et al., 2009, Martí et al., 2016]. The performance of a two-start based approach is $\mathbb{E}_{X, \hat{\theta}_0, \hat{\theta}_1}[\min\{\hat{Y}_0, \hat{Y}_1\}]$. From Proposition 2, if the initializer $\tilde{\theta}$ can order the two points sufficiently accurately, i.e. γ is high, then the performance of initialization is close to the multi-start based approach. Next, we construct an initializer inspired from Proposition 1 and 2 that sequentially initializes GD to solve problem instances $\{X_i\}_{i=1}^{\infty}$.

How can we construct initializers that are better than independent random initializer?

Vanilla approach. For an incoming instance X , sample $\hat{\theta}_0$ and $\hat{\theta}_1$ from $\mathbb{P}_{\hat{\theta}}$, compute the solutions \hat{Y}_0 and \hat{Y}_1 respectively using GD and select the solution with a smaller objective value. Repeat this for first N instances. Train a model Ψ that takes as input $X, \hat{\theta}_0, \hat{\theta}_1$ and outputs a real value to predict $\hat{Y}_1 - \hat{Y}_0$. For every new X , sample $\hat{\theta}_0$ and $\hat{\theta}_1$. Define a Bernoulli Z_{vanilla} with $p_{\text{vanilla}}(\hat{\theta}_0, \hat{\theta}_1, X) = \frac{e^{\Psi(\hat{\theta}_0, \hat{\theta}_1, X)}}{1 + e^{\Psi(\hat{\theta}_0, \hat{\theta}_1, X)}}$ as the probability $Z_{\text{vanilla}} = 0$ and initialize from $\tilde{\theta}_{\text{vanilla}} = (1 - Z_{\text{vanilla}})\hat{\theta}_0 + Z_{\text{vanilla}}\hat{\theta}_1$. Define the corresponding solution value $\tilde{Y}_{\text{vanilla}} = (1 - Z_{\text{vanilla}})\hat{Y}_0 + Z_{\text{vanilla}}\hat{Y}_1$. The Pearson correlation between random variables U, V is $\rho(U, V)$.

Proposition 3. (*Vanilla vs. independent random*) If $\rho(p_{\text{vanilla}}(\hat{\theta}_0, \hat{\theta}_1, X), \hat{Y}_1 - \hat{Y}_0) > 0$, then the Vanilla approach performs better than the independent random initializer, i.e., $\mathbb{E}_{X, \tilde{\theta}_{\text{vanilla}}}[\tilde{Y}_{\text{vanilla}}] < \mathbb{E}_{X, \hat{\theta}}[\hat{Y}]$.

Since the model Ψ tries to predict $\hat{Y}_1 - \hat{Y}_0$, we expect a positive correlation between Ψ and $\hat{Y}_1 - \hat{Y}_0$. As p_{vanilla} is an increasing invertible transformation of Ψ , we expect a positive correlation between p_{vanilla} and $\hat{Y}_1 - \hat{Y}_0$ (see Appendix for details). Proposition 3 is reminiscent of the following result in binary classification: as long as a classifier's output is positively correlated with the binary label, the classifier performs better than a uniformly random classifier (see Appendix for details). The Vanilla approach only works with two initial values and requires access to the outcomes from multiple initializations for the same problem instance. Next, we propose a more general approach next that works with multiple initial values and also does not require access to multiple outcomes for the same instance.

Algorithm 2 Val-Init and Arg-Init Methods

Input: Instances $\{X_i\}_{i=1}^\infty \sim \mathbb{P}_X$, \mathcal{H}_{val} , \mathcal{H}_{arg} Hypothesis classes for h_{val} , h_{arg} respectively

for $i \in \{1, \dots, \infty\}$ **do**

if $i \leq N$ **then**

$\hat{\theta}^i \sim \mathbb{P}_{\hat{\theta}}, f_i = f(\cdot, X_i)$, $\hat{\theta}_i^\dagger, \hat{Y}_i \xleftarrow{\text{Alghm8}} \text{GD}(f_i, \hat{\theta}^i)$,

end if

$h_{\text{val}} = \arg \min_{h \in \mathcal{H}_{\text{val}}} \sum_{j=1}^N \ell(h(\hat{\theta}^j, X_j), \hat{Y}_j)$

$h_{\text{arg}} = \arg \min_{h \in \mathcal{H}_{\text{arg}}} \sum_{j=1}^N \ell(h(\hat{\theta}^j, X_j), \hat{\theta}_j^\dagger)$

if $i \geq N + 1$ **then**

$\{\hat{\theta}_m^i \sim \mathbb{P}_{\hat{\theta}}\}_{m=0}^{M-1}$,

$m^* = \arg \min \{h_{\text{val}}(\hat{\theta}_m^i, X_i)\}_{m=0}^{M-1}$,

$\tilde{\theta}_{\text{val}} = \hat{\theta}_{m^*}^i, f_i = f(\cdot, X_i)$,

$\tilde{\theta}_{\text{val}}, \tilde{Y}_{\text{val}} = \text{GD}(f_i, \hat{\theta}_{m^*}^i)$

$\tilde{\theta}_{\text{arg}}, \tilde{Y}_{\text{arg}} = \text{GD}(f_i, h_{\text{arg}}(\hat{\theta}_0^i, X_i))$

end if

end for

3.2 Val-Init: Learn from solution values

The approach is divided into two phases. In the first phase comprising N instances, we find the solution for the i^{th} instance X_i using random initialization $\hat{\theta} \sim \mathbb{P}_{\hat{\theta}}$. In the second phase, we learn a model $h_{\text{val}} : \mathbb{R}^m \times \mathbb{R}^n \rightarrow \mathbb{R}$ to predict for initialization $\hat{\theta}$ and instance X_i the objective value at solution $g(\hat{\theta}, X_i)$. We use the learned model h_{val} to select initializations as follows. For each new instance, generate M i.i.d. random initializations $\{\hat{\theta}_k\}_{k=0}^{M-1}$ from $\mathbb{P}_{\hat{\theta}}$ and compute the predicted value of the final solution using h_{val} . Select the initialization with lowest predicted value. We provide the algorithmic description in Algorithm 2; we refer to the approach as Val-Init as it uses the predicted values to initialize. We define some random variables to describe the Val-Init initializer. Define $\{Z_k\}_{k=0}^{M-1}$ as M random variables, where each $Z_k \in \{0, 1\}$ and $\sum_{k=0}^{M-1} Z_k = 1$. If $\arg \min \{h_{\text{val}}(X, \hat{\theta}_k)\}_{k=0}^{M-1} = j$, then $Z_j = 1$, else $Z_j = 0$, thus Z_j indicates the initializer selected. Define the Val-Init initializer as $\tilde{\theta}_{\text{val}} = \sum_{k=0}^{M-1} Z_k \hat{\theta}_k$ and the corresponding solution value as $\tilde{Y}_{\text{val}} = \sum_{k=0}^{M-1} Z_k \hat{Y}_k$, where $\hat{Y}_k = g(X, \hat{\theta}_k)$ is the solution value achieved from $\hat{\theta}_k$.

Proposition 4. (*Val-Init vs. independent random*) If $\rho(Z_k, \hat{Y}_{M-1} - \hat{Y}_k) > 0 \forall k \in \{0, \dots, M-2\}$, then Val-Init performs better than the independent random initializer, i.e., $\mathbb{E}_{X, \tilde{\theta}_{\text{val}}}[\tilde{Y}_{\text{val}}] < \mathbb{E}_{X, \hat{\theta}}[\hat{Y}]$.

From the above Proposition it follows that if the objective value \hat{Y}_k is small, then we expect the corresponding selection variable Z_k to be large.

How does Val-Init compare to M multi-starts?

Define the set of objective function values achievable from all possible initializations for an instance x as $\mathcal{F}(x)$. For each problem instance x , define a mapping Φ_x that maps a real input value y to the set of initializations from which y can be achieved using GD.

Assumption 3. (*Minimum separation*) For an $x \in \mathcal{X}$, if $y \in \mathcal{F}(x)$, $z \in \mathcal{F}(x)$, $y \neq z$, then $\exists \Delta > 0$ s.t. $|y - z| \geq \Delta$.

If GD arrives at a finite set of distinct values from all initializations, then the above assumption holds.

Assumption 4. (*Bounded error*) Consider a problem instance $x \in \mathcal{X}$. For each y which satisfies $\mathbb{P}_{\hat{\theta}}(\hat{\theta} \in \Phi_x(y)) > 0$, $\mathbb{E}_{\hat{\theta}}[|y - h_{\text{val}}(\hat{\theta}, x)|^2 | \hat{\theta} \in \Phi_x(y), X = x] \leq \frac{\Delta^2 \zeta}{4}$, where $0 < \zeta < \frac{\tilde{\epsilon}}{M f^{\text{sup}}}$ and $f^{\text{sup}} = \sup_{\theta \in \Theta} f(\theta, x) < \infty$ and $\tilde{\epsilon} > 0$ is a small positive quantity.

Assumption 4 requires the prediction error of h_{val} to be bounded. The bound is not restrictive, especially if Δ (the difference between distinct objective values at solution) is not small.

Proposition 5. (*Val-Init vs. M multi-starts*) For problem instance x , if Assumptions 3 and 4 hold, then Val-Init is an $\tilde{\epsilon}$ -approximation of the multi-start approach:

$$\mathbb{E}_{\{\hat{\theta}_k\}_{k=0}^{M-1}}[\tilde{Y}_{\text{val}} | X = x] \leq \mathbb{E}_{\{\hat{\theta}_k\}_{k=0}^{M-1}}[\min_{k \in \{0, \dots, M-1\}} \{\hat{Y}_k\} | X = x] + \tilde{\epsilon}.$$

From the above Proposition, Val-Init can perform close to the multi-start based approach without running GD multiple times from different start points for same problem instance. Note that Val-Init learns from the solution’s function values. Next, we propose an approach that learns from the solution’s argument values.

3.3 Arg-Init: Learn from solution arguments

This approach also consists of two phases. The first phase of this approach is identical to the first phase of Val-Init: we collect data using random initializations. In the second phase, we learn a model $h_{\text{arg}} : \mathbb{R}^m \times \mathbb{R}^n \rightarrow \mathbb{R}^m$ that maps the initialization $\hat{\theta}$ and the instance X to predict the solution argument $g^\dagger(\hat{\theta}, X)$ (output of GD defined in Section 2). For each new instance X , sample $\hat{\theta} \sim \mathbb{P}_{\hat{\theta}}$ and input it to the learned model h_{arg} to generate the initialization point $h_{\text{arg}}(\hat{\theta}, X)$. We provide the algorithmic description in Algorithm 2; we refer to this approach as Arg-Init as it uses solution arguments to initialize. Arg-Init predicts an initialization, which it hopes is closer to the solution of a random initialization $\hat{\theta}$ as that can lead to faster convergence. Define this condition as an event called “ η -factor reduction” given as $\|h_{\text{arg}}(\hat{\theta}, X) - g^\dagger(\hat{\theta}, X)\| \leq \eta \|\hat{\theta} - g^\dagger(\hat{\theta}, X)\|$, where $\eta < 1$. See Appendix for how this event leads to η -factor reduction in the number of iterations to convergence.

Assumption 5. (*Uniform continuity of $\mathbb{P}_{\hat{\theta}}$*) For each $\epsilon > 0$, \exists a δ such that for any θ in the interior of Θ and a ball $B_\delta = \{\bar{\theta} \in \Theta \mid \|\bar{\theta} - \theta\| \leq \delta\}$ of radius δ around θ^\dagger the probability $\mathbb{P}_{\hat{\theta}}(\hat{\theta} \in B_\delta) \leq \epsilon$.

Proposition 6. (*Arg-Init vs. independent random*) If Assumption 5 holds and the prediction error of h_{arg} is small, i.e. $0 < s < 1$, $0 < \eta < 1$, $\mathbb{E}_{X, \hat{\theta}}[\|h_{\text{arg}}(\hat{\theta}, X) - g^\dagger(\hat{\theta}, X)\|^2] \leq s(1 - \epsilon)(\delta\eta)^2$, where ϵ, δ are from Assumption 5, then with probability $(1 - s)(1 - \epsilon)$ Arg-Init achieves η -factor reduction.

If ϵ decreases, then δ in Assumption 5 decreases, the upper bound on the error in the Proposition 6 should decrease and the probability of η -factor reduction increases. Before we proceed to the experiments, we close with a comparison of Arg-Init and Val-Init in Figure 1. We expect Arg-Init to work in both convex and non-convex problems. Since Val-Init is based on comparing local minima (stationary points) it is not suited for convex problems. Val-Init it can offer advantage over Arg-Init whenever the local minima values differ substantially (as shown in Figure 1 and Ackley function experiment Section 4). From a learning point of view Val-Init 2 needs to learn a function with scalar output, while Arg-Init needs to learn a function with output dimesions same as the optimization variable θ .

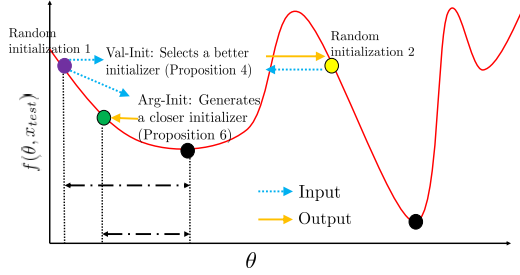


Figure 1: Arg-Init vs. Val-Init overview

4 Experiments

In this section, we apply our methods (Val-Init and Arg-Init) to solve various optimization problems. We first illustrate our methods on a standard non-convex optimization problem. (We also provide synthetic convex optimization experiments in the Appendix.) We then illustrate our methods on real applications such as generating adversarial examples, generating contrastive explanations, and sum-rate optimization. We compare our initialization methods with the random initialization, zero initialization, and initializers learned using a MAML-based approach [Finn et al., 2017]. For all methods, the choice of architectures, hyperparameters, train and test sizes, validation error of h_{val} and h_{arg} (during training) are in the Appendix. We use all the initialization methods as single-start methods (comparing single-start with multi-start is not fair as multi-start method has a higher computational cost). For each problem family (generate explanations for a model), we are provided different problem instances (data points) and we need to generate solutions to them (explanations). For each problem instance, we initialize gradient descent using different initialization methods to search the solutions. The performance is defined as the average of the objective function values (at the solution) across different problem instances. We compare the methods in terms of the performance achieved vs. the number of iterations of gradient descent. Histograms showing the distribution of performance across problem instances is in the Appendix.

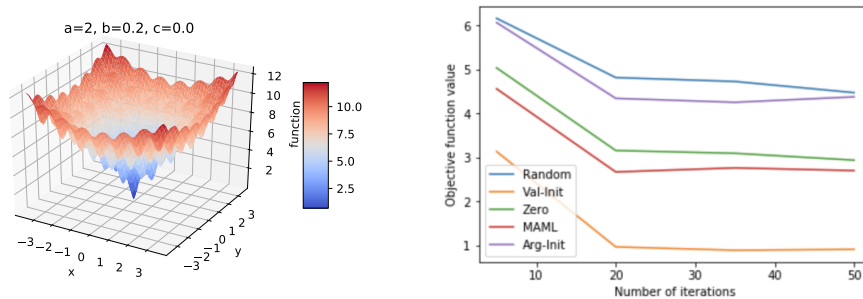


Figure 2: Illustration of Ackley function (left), and objective function value vs. number of iterations (right)

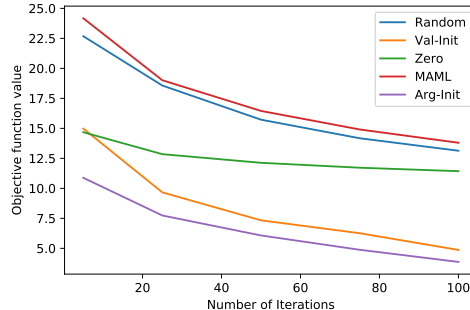


Figure 3: Adversarial examples on CIFAR-10: Objective function value vs. number of iterations

4.1 Ackley function minimization

Ackley functions are used to study non-convex optimization problems [Ackley, 2012]. Ackley function is defined as $A(x, y, a, b, c) = -a \exp(-b \frac{\sqrt{(x-c)^2 + (y-c)^2}}{2}) - \exp(\frac{\cos(2\pi(x-c)) + \cos(2\pi(y-c))}{2}) + \exp(1) + a$. The global minimum of the function is at (c, c) and the minimum value is zero. In Figure 2, we show an instantiation of Ackley function. The function has many minima that are worse than the global minimum. We are given a set of Ackley functions with parameters a, b, c drawn i.i.d. from $a \sim 20 + U[0, 10]$, $b \sim 0.2 + U[0, 0.1]$, and $c \sim U[0, 2]$, where U is a uniform distribution. We want to learn an initializer that takes a, b, c as input and generates an initialization. We train Arg-Init, Val-Init (Algorithm 2) using 1500 i.i.d draws of a, b, c from the above uniform distributions. In Figure 2, we compare the methods in terms of the average objective function value vs. iterations in gradient descent, where the average is taken over 500 unseen instances a, b, c . Val-Init performs better across different iteration values. Arg-Init did not generate a good initialization in this case suggesting Val-Init is potentially more useful in highly non-convex problems.

4.2 Datasets, models for adversarial examples and contrastive explanations

CIFAR-10. We trained a convolutional neural network (on the default train-test split of CIFAR-10) that achieves 70% accuracy in predicting the classes.

MNIST. We trained a 2 layer neural network (on the default train-test split of MNIST digits) that achieves 97% accuracy in predicting the digits.

Waveform. The dataset consists of 40 attributes that help identify the wave type (from three types of waves). We divided the data into 75% training and 25% testing. We trained a 2 layer neural network that achieves 85% accuracy to predict the wave type.

HELOC. Home equity line of credit (HELOC) data contains the information about the applicant in their credit report and their loan repayment history. We build a model to predict whether applicants will make timely payments. We divided the data into 75% training and 25% testing. We trained a 2 layer neural network using the training data that achieves 72% accuracy in predicting repayments.

For each model trained above and the respective train split, we run gradient descent with random initialization to generate adversarial example (contrastive explanation) for each point in the train split and learn h_{val} and h_{arg} . Next, for each point in the respective test split we run gradient descent

Table 1: **Adversarial examples.** Comparing performance in terms of the penalty-based objective. Average distance value, the fraction of instances when constraints are not satisfied are mentioned below the penalty-based objective value. The best methods in terms of the penalty-based objective are in bold. All methods are run for 100 iterations in Waveform and MNIST and 10 iterations in HELOC.

METHOD	HELOC	WAVEFORM	MNIST
ARG-INIT	-0.37 (0.44, 0.016)	-0.89 (0.45, 0.03)	1.66 (1.15, 0.17)
VAL-INIT	1.39 (1.85, 0.25)	-0.67 (0.85, 0.22)	0.98 (0.81, 0.00)
RANDOM	1.42 (1.86, 0.26)	-0.66 (0.85, 0.21)	3.41 (1.90, 0.00)
ZERO	0.021 (0.50, 0.013)	-0.89 (0.32, 0.09)	4.60 (0.97, 0.02)
MAML	-0.017 (0.94, 0.00)	-0.89 (0.69, 0.00)	7.09 (3.76, 0.00)

with different initializers to generate adversarial example (contrastive explanations). We compare the methods in terms of the average quality of the adversarial examples (explanations) across the test instances. Details on the objective used for gradient descent are provided next.

4.3 Adversarial examples

Recall, if $\beta = 0$ and $\Theta = \mathbb{R}^m$ in equation (2), we obtain the problem of finding an adversarial example for a binary classifier. We then reformulate equation (2) into a commonly used penalty-based objective as follows $\|\theta\| + \mathcal{L}(y(u(x + \theta)))$ (\mathcal{L} is from equation 3 in [Cheng et al., 2018]). We compare all the methods in terms of this penalized objective function as it reflects the quality of the adversarial example. In Figure 3, we compare the performance of the methods (penalized objective averaged across test instances in the data) vs. the number of iterations in gradient descent. Arg-Init is the best closely followed by Val-Init. Except for zero initialization, every method was able to generate an example from a different class than the data instance, i.e., satisfy the constraint in equation (2), for each input instance. Before moving to next comparisons, we contrast the validation mean square error at the end of first last epoch in training to show that even in a relatively more complex setting of CIFAR-10 it is possible to learn h_{val} (1 million parameters) and h_{arg} (1.5 million parameters). We find that validation MSE values decrease from 47.68 to 24.92 and from 0.0244 to 0.0171 for h_{val} and h_{arg} respectively. We provide these values for all the other experiments in the Appendix. For other datasets we provide a table of comparisons (Table 1) for a fixed number of iterations and the plots for objective vs. iterations are given in the Appendix. In Table 1, we see that Val-Init is the best on MNIST, Arg-Init is the best on HELOC, and Arg-Init is tied with Zero and MAML on Waveform.

In Figure 4, we contrast our approach to random initialization for adversarial examples on MNIST.

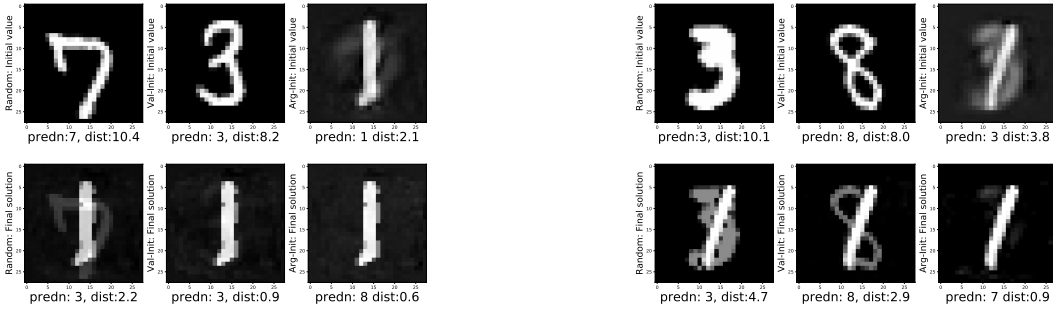
Table 2: **Contrastive examples.** Comparing performance in terms of the penalty-based objective defined in [Dhurandhar et al., 2018]. Average distance value, the fraction of instances when constraints are not satisfied are mentioned below the objective value. The best methods in terms of the optimization objective are in bold. All methods are run for 100 iterations in Waveform and MNIST and 10 iterations in HELOC.

METHOD	WAVEFORM	MNIST
ARG-INIT	0.40 (0.42, 0.19)	-0.03 (0.93, 0.02)
VAL-INIT	2.23 (1.95, 0.23)	0.54 (2.16, 0.01)
RANDOM	3.51 (1.95, 0.44)	1.49 (3.90, 0.00)
ZERO	0.61 (0.36, 0.23)	4.29 (0.95, 0.69)
MAML	0.40 (0.41, 0.19)	2.32 (4.56, 0.00)

The final solutions shown all satisfy the constraint that they are classified from a different class than the original image’s class 1. The solution generated from our approach is visually indistinguishable from class 1, while that is not the case for the solution generated from random approach. We found this to be the case across most examples. In Figure 4, we also do a visual contrast of the initial values used by Val-Init, Arg-Init, and random initialization. Our approaches finds points that morph easily into class 1 (class for which adversarial examples are generated).

4.4 Contrastive explanations (PNs)

Recall, if $\beta > 0$ and Θ is constrained to PNs [Dhurandhar et al., 2018] in equation (2), we obtain the problem of finding PNs based explanations. We then reformulate equation (2) into a penalty-based objective minimization in [Dhurandhar et al., 2018]. We compare the methods in terms of the average penalty-based objective. No PNs were found in the HELOC data and the PN framework does not apply to colored images as in CIFAR-10, thus no comparisons were possible on HELOC and CIFAR-10 dataset. In Table 2, we summarize the comparisons. On MNIST digits, Arg-Init is the best and Val-Init also does well in generating PNs. On Waveform, Arg-Init and MAML perform the best. In Figure 4, we contrast our approaches to random initialization for PNs on MNIST. The final solutions shown satisfy the constraint that they are classified from a different class than the original image’s class 1. The solution generated from our approach are sparser and thus better PNs; this is true across many examples. In Figure 4, we also show the initial values used. Our approaches start from points that easily morph into sparse PNs.



a. Adversarial examples

b. Contrastive explanations

Figure 4: Comparing solution quality for different initializations for same iterations. Top row: initializations, bottom row: respective final solns. Left column (random), middle column (Val-Init), right column (Arg-Init). Below each image we state predicted class & distance from original instance.

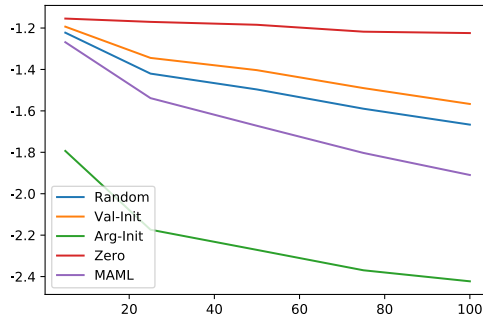


Figure 5: $-\text{Sum rate}$ vs. number of iterations

4.5 Sum-rate optimization

We compare the different approaches to initialize gradient descent to solve the sum-rate optimization problem (described in Section 2). We train Val-Init and Arg-Init using 5000 problem instances (solved using gradient descent with random initialization) for 15 users. Each problem instance is a new independent draw of the channel matrix from a standard uniform random distribution (each element in the matrix is i.i.d. drawn from uniform distribution over $[0,10]$). We test on the 500 instances from the same distribution; see Figure 5 for comparisons. Arg-Init beats all methods (25 % gain).

4.6 Overall comparison summary

Let us start with Arg-Init approach. In seven out of the eight instances, it is at least as good (two times) or better (five times) than all the existing methods. Next, consider the Val-Init approach. It performs better than the existing methods in four out of eight instances. Recall the Val-Init is not designed for problems where the local minimum values do not differ by a lot for e.g., convex

optimization problems, where all the minima take the same value. In the instances where Val-Init did not outperform others – tabular datasets for adversarial examples and sum-rate optimization – it is possible that the different local-minimum values do not differ by a lot thus not giving much room for Val-Init method to perform well. In contrast, see the example of Ackley function and relatively more complex datasets such as CIFAR-10 and MNIST, Val-Init was able to exploit the variance in different local minimum values.

5 Conclusion

In optimization solvers that use gradient descent, initialization is crucial to finding “good” local minima. Therefore, it is common practice to hand-engineer initialization rules. In this work, we developed theory that led to two approaches that learn how to initialize for an input problem class. The first approach learns to discriminate different initial values and selects the best, and the second uses an initial value to create another value that is closer to the local minima. We carried out experiments on several datasets (real and synthetic) and on a variety of optimization problems (convex and non-convex) where at least one of these simple approaches has state-of-the-art performance. In the future, it would be interesting to extend these approaches to more general settings (viz. initializing NNs) with the possibility of even intelligently combining them.

6 Appendix

We organize the Appendix as follows. In the first section, we provide the proofs to all the propositions. In the second section, we provide supplementary materials for the experiments.

6.1 Proofs

In this section, we provide the proofs to the propositions. We restate the propositions for reader’s convenience. We restate Proposition 1 below.

Proposition 7. *Assumption 1* $\iff \mathbb{E}_{X,\hat{\theta}}[\tilde{Y}] < \mathbb{E}_{X,\hat{\theta}}[\hat{Y}]$

Proof. Let us first simplify $\mathbb{E}_{X,\hat{\theta}}[\tilde{Y}]$

$$\begin{aligned}
\mathbb{E}_{X,\hat{\theta}}[\tilde{Y}] &= \mathbb{E}_{X,\hat{\theta}}[g(\tilde{\theta}, X)] \\
&= \mathbb{E}_{X,\hat{\theta}}[g((1-Z)\hat{\theta}_0 + Z\hat{\theta}_1, X)] \\
&= \mathbb{E}_{X,\hat{\theta}}[(1-Z)g(\hat{\theta}_0, X) + Zg(\hat{\theta}_1, X)] \\
&= \mathbb{E}_{X,\hat{\theta}_0,\hat{\theta}_1,Z}[(1-Z)g(\hat{\theta}_0, X) + Zg(\hat{\theta}_1, X)] \\
&= \mathbb{E}_{X,\hat{\theta}_0,\hat{\theta}_1}[(1 - \mathbb{E}_{Z|X,\hat{\theta}_0,\hat{\theta}_1}[Z])g(\hat{\theta}_0, X) + \mathbb{E}_{Z|X,\hat{\theta}_0,\hat{\theta}_1}[Z]g(\hat{\theta}_1, X)] \\
&= \mathbb{E}_{X,\hat{\theta}_0,\hat{\theta}_1}[p(\hat{\theta}_0, \hat{\theta}_1, X)g(\hat{\theta}_0, X) + (1 - p(\hat{\theta}_0, \hat{\theta}_1, X))g(\hat{\theta}_1, X)]
\end{aligned} \tag{3}$$

Since $\hat{\theta}_0$ and $\hat{\theta}_1$ are identical draws from $\mathbb{P}_{\hat{\theta}}$ we obtain

$$\mathbb{E}_{X,\hat{\theta}_1}[g(\hat{\theta}_1, X)] = \mathbb{E}_{X,\hat{\theta}_0}[g(\hat{\theta}_0, X)] = \mathbb{E}_{X,\hat{\theta}}[g(\hat{\theta}, X)] = \mathbb{E}_{\hat{\theta},X}[\hat{Y}] \tag{4}$$

Therefore, we can use the above condition (4) to obtain

$$\mathbb{E}_{X,\hat{\theta}}[\hat{Y}] = \mathbb{E}_{X,\hat{\theta}_0,\hat{\theta}_1}\left[\frac{1}{2}g(\hat{\theta}_0, X) + \frac{1}{2}g(\hat{\theta}_1, X)\right] \quad (5)$$

Take the difference of LHS of (3) and (5) to obtain

$$\mathbb{E}_{X,\tilde{\theta}}[\tilde{Y}] - \mathbb{E}_{X,\hat{\theta}}[\hat{Y}] = \mathbb{E}_{X,\hat{\theta}_0,\hat{\theta}_1}\left[\left(p(\hat{\theta}_0, \hat{\theta}_1, X) - \frac{1}{2}\right)(g(\hat{\theta}_0, X) - g(\hat{\theta}_1, X))\right] \quad (6)$$

Therefore, $\mathbb{E}_{X,\hat{\theta}_0,\hat{\theta}_1}\left[\left(p(\hat{\theta}_0, \hat{\theta}_1, X) - \frac{1}{2}\right)(g(\hat{\theta}_0, X) - g(\hat{\theta}_1, X))\right] < 0 \iff \mathbb{E}_{X,\tilde{\theta}}[\tilde{Y}] - \mathbb{E}_{X,\hat{\theta}}[\hat{Y}] < 0$ This proves the theorem. \square

We restate Proposition 2 below.

Proposition 8. *Assumption 2* $\implies \mathbb{E}_{X,\hat{\theta}_0,\hat{\theta}_1}[\min\{\hat{Y}_0, \hat{Y}_1\}] \leq \mathbb{E}_{X,\tilde{\theta}}[\tilde{Y}] \leq \gamma\mathbb{E}_{X,\hat{\theta}_0,\hat{\theta}_1}[\min\{\hat{Y}_0, \hat{Y}_1\}] + (1 - \gamma)\mathbb{E}_{X,\hat{\theta}_0,\hat{\theta}_1}[\max\{\hat{Y}_0, \hat{Y}_1\}]$

Proof. From (3) it follows that

$$\mathbb{E}_{X,\tilde{\theta}}[\tilde{Y}] = \mathbb{E}_{X,\hat{\theta}_0,\hat{\theta}_1}[p(\hat{\theta}_0, \hat{\theta}_1, X)\hat{Y}_0 + (1 - p(\hat{\theta}_0, \hat{\theta}_1, X))\hat{Y}_1] \quad (7)$$

Consider the term inside the expectation given above.

Suppose $\hat{Y}_0 \leq \hat{Y}_1$ then from Assumption 2 it follows

$$p(\hat{\theta}_0, \hat{\theta}_1, X)\hat{Y}_0 + (1 - p(\hat{\theta}_0, \hat{\theta}_1, X))\hat{Y}_1 \leq \gamma\hat{Y}_0 + (1 - \gamma)\hat{Y}_1 \quad (8)$$

Suppose $\hat{Y}_1 < \hat{Y}_0$ then from Assumption 2 it follows

$$p(\hat{\theta}_0, \hat{\theta}_1, X)\hat{Y}_0 + (1 - p(\hat{\theta}_0, \hat{\theta}_1, X))\hat{Y}_1 \leq \gamma\hat{Y}_1 + (1 - \gamma)\hat{Y}_0 \quad (9)$$

Combining equations (8) and (9), we get

$$\begin{aligned} &\mathbb{E}_{X,\hat{\theta}_0,\hat{\theta}_1}[p(\hat{\theta}_0, \hat{\theta}_1, X)\hat{Y}_0 + (1 - p(\hat{\theta}_0, \hat{\theta}_1, X))\hat{Y}_1] \leq \\ &\gamma\mathbb{E}_{X,\hat{\theta}_0,\hat{\theta}_1}[\min\{\hat{Y}_0, \hat{Y}_1\}] + (1 - \gamma)\mathbb{E}_{X,\hat{\theta}_0,\hat{\theta}_1}[\max\{\hat{Y}_0, \hat{Y}_1\}] \end{aligned} \quad (10)$$

LHS of the above Proposition follows trivially. Observe that \tilde{Y} takes one of the values \hat{Y}_0 or \hat{Y}_1 . Therefore, $\min\{\hat{Y}_0, \hat{Y}_1\} \leq \tilde{Y} \implies \mathbb{E}_{X,\hat{\theta}_0,\hat{\theta}_1}[\min\{\hat{Y}_0, \hat{Y}_1\}] \leq \mathbb{E}_{X,\hat{\theta}_0,\hat{\theta}_1}[\tilde{Y}]$. \square

We restate Proposition 3 below.

Proposition 9. *If $\rho(p_{\text{vnila}}(\hat{\theta}_0, \hat{\theta}_1, X), \hat{Y}_1 - \hat{Y}_0) > 0$, then the Vanilla approach performs better than the independent random initializer, i.e., $\mathbb{E}_{X,\hat{\theta}_{\text{vnila}}}[\tilde{Y}_{\text{vnila}}] < \mathbb{E}_{X,\hat{\theta}}[\hat{Y}]$.*

Proof. Since the Pearson correlation is positive $\mathbb{E}_{X,\hat{\theta}_0,\hat{\theta}_1}\left[(p(\hat{\theta}_0, \hat{\theta}_1, X))(\hat{Y}_1 - \hat{Y}_0)\right] > 0 \implies \mathbb{E}_{X,\hat{\theta}_0,\hat{\theta}_1}\left[\left(p(\hat{\theta}_0, \hat{\theta}_1, X) - \frac{1}{2}\right)(\hat{Y}_0 - \hat{Y}_1)\right] < 0$ where we use the fact $\mathbb{E}[\hat{Y}_0 - \hat{Y}_1] = 0$. The rest follows from Proposition 1. \square

We restate Proposition 4 below.

Proposition 10. *If $\rho(Z_k, \hat{Y}_{M-1} - \hat{Y}_k) > 0 \forall k \in \{0, \dots, M-2\}$, then Val-Init performs better than the independent random initializer, i.e., $\mathbb{E}_{X, \tilde{\theta}_{\text{val}}}[\tilde{Y}_{\text{val}}] < \mathbb{E}_{X, \hat{\theta}}[\hat{Y}]$.*

Proof. Simplify $g(\tilde{\theta}_{\text{val}}, X)$ to obtain

$$\tilde{Y}_{\text{val}} = g(\tilde{\theta}_{\text{val}}, X) = g\left(\sum_{k=0}^{M-1} Z_k \hat{\theta}_k, X\right) = \sum_{k=0}^{M-1} Z_k g(\hat{\theta}_k, X) = \sum_{k=0}^{M-1} Z_k \hat{Y}_k \quad (11)$$

Define a discrete uniform random variable W that takes one of the values in the set $\{0, \dots, M-1\}$. Define R_k as a random variable which indicates if $W = k$, i.e., if $W = k$, then $R_k = 1$, else it is zero. Observe that $\sum_{k=0}^{M-1} R_k = 1$. Define the objective value achieved by random initializer as $\hat{Y} = \sum_{k=0}^{M-1} R_k \hat{Y}_k$. Take the difference between \tilde{Y}_{val} and \hat{Y} to obtain

$$\begin{aligned} \tilde{Y}_{\text{val}} - \hat{Y} &= \sum_{k=0}^{M-1} (Z_k - R_k) \hat{Y}_k \\ &= \sum_{k=0}^{M-2} (Z_k - R_k) \hat{Y}_k + (Z_{M-1} - R_{M-1}) \hat{Y}_{M-1} \\ &= \sum_{k=0}^{M-2} (Z_k - R_k) (\hat{Y}_k - \hat{Y}_{M-1}) \end{aligned} \quad (12)$$

In the above simplification, we used $R_{M-1} = 1 - \sum_{k=0}^{M-2} R_k$ and $Z_{M-1} = 1 - \sum_{k=0}^{M-2} Z_k$. Recall that the correlation between two random variables X and Y is given as $\rho(X, Y) = \frac{E[XY] - E[X]E[Y]}{\sigma_X \sigma_Y}$, where σ_X and σ_Y is the standard deviation of X and Y . We use this identity in our simplification next.

Let us consider the expectation of one of the terms inside the summation above (12)

$$\begin{aligned} \mathbb{E}[(Z_k - R_k)(\hat{Y}_k - \hat{Y}_{M-1})] &= \\ \mathbb{E}[(Z_k - R_k)]\mathbb{E}[(\hat{Y}_k - \hat{Y}_{M-1})] + \rho(Z_k - R_k, \hat{Y}_k - \hat{Y}_{M-1})\sigma_{Z_k - R_k}\sigma_{\hat{Y}_k - \hat{Y}_{M-1}} &= \\ \rho(Z_k - R_k, \hat{Y}_k - \hat{Y}_{M-1})\sigma_{Z_k - R_k}\sigma_{\hat{Y}_k - \hat{Y}_{M-1}} &< 0 \end{aligned} \quad (13)$$

In the above simplification (13), we use the following facts i) $\mathbb{E}[(\hat{Y}_k - \hat{Y}_{M-1})] = 0$ because \hat{Y}_k and \hat{Y}_{M-1} are identically distributed, ii) the correlation $\rho(Z_k - R_k, \hat{Y}_k - \hat{Y}_{M-1}) < 0$, and iii) standard deviations $\sigma_{Z_k - R_k}$, $\sigma_{\hat{Y}_k - \hat{Y}_{M-1}}$ are positive. \square

Lemma 1. *If Assumption 4 holds, then*

$$\mathbb{P}_{\theta}\left(|y - h_{\text{val}}(\hat{\theta}, x)| < \Delta/2 \mid \hat{\theta} \in \Phi_x(y), X = x\right) > 1 - \zeta \quad (14)$$

Proof. We rewrite the probability in the lemma as follows

$$\begin{aligned}
& \mathbb{P}_{\hat{\theta}}\left(|y - h_{\text{val}}(\hat{\theta}, x)| < \Delta/2 \mid \hat{\theta} \in \Phi_x(y), X = x\right) \\
&= \mathbb{P}_{\hat{\theta}}\left(|y - h_{\text{val}}(\hat{\theta}, x)|^2 < \Delta^2/4 \mid \hat{\theta} \in \Phi_x(y), X = x\right) \\
&= 1 - \mathbb{P}_{\hat{\theta}}\left(|y - h_{\text{val}}(\hat{\theta}, x)|^2 \geq \Delta^2/4 \mid \hat{\theta} \in \Phi_x(y), X = x\right)
\end{aligned} \tag{15}$$

We simplify the second term in the last expression above (15) using Markov's inequality

$$\begin{aligned}
& \mathbb{P}_{\hat{\theta}}\left(|y - h_{\text{val}}(\hat{\theta}, x)|^2 \geq \Delta^2/4 \mid \hat{\theta} \in \Phi_x(y), X = x\right) \leq \\
& \frac{\mathbb{E}[|y - h_{\text{val}}(\hat{\theta}, x)|^2 \mid \hat{\theta} \in \Phi_x(y), X = x]}{\Delta^2/4}
\end{aligned} \tag{16}$$

We use Assumption 4 to simplify (16) as follows

$$\frac{\mathbb{E}[|y - h_{\text{val}}(\hat{\theta}, x)|^2 \mid \hat{\theta} \in \Phi_x(y), X = x]}{\Delta^2/4} \leq \frac{\Delta^2/4(\zeta)}{\Delta^2/4} \leq \zeta \tag{17}$$

From (16) and (17), it follows that

$$\mathbb{P}_{\theta}\left(|y - h_{\text{val}}(\hat{\theta}, x)|^2 \geq \Delta^2/4 \mid \hat{\theta} \in \Phi_x(y), X = x\right) \leq \zeta < \frac{\tilde{\epsilon}}{M f^{\text{sup}}} \tag{18}$$

From (15) it follows that

$$\mathbb{P}_{\theta}\left(|y - h_{\text{val}}(\hat{\theta}, x)| < \Delta/2 \mid \hat{\theta} \in \Phi_x(y), X = x\right) > 1 - \frac{\tilde{\epsilon}}{f^{\text{sup}}M} \tag{19}$$

This completes the proof. \square

We restate Proposition 5 below.

Proposition 11. *For problem instance x , if Assumptions 3 and 4 hold, then Val-Init is an $\tilde{\epsilon}$ -approximation of the multi-start based approach:*

$$\mathbb{E}_{\{\hat{\theta}_k\}_{k=0}^{M-1}}[\tilde{Y}_{\text{val}} \mid X = x] \leq \mathbb{E}_{\{\hat{\theta}_k\}_{k=0}^{M-1}}\left[\min_{k \in \{0, \dots, M-1\}} \{\hat{Y}_k\} \mid X = x\right] + \tilde{\epsilon}.$$

Proof. We will consider the case when $M = 2$. The same steps of the proof can be repeated for the general case when $M > 2$. We can write $\tilde{Y}_{\text{val}} = (1 - Z)\hat{Y}_0 + Z\hat{Y}_1$, where Z is the selection variable decided by Val-Init algorithm.

$$\begin{aligned}
\mathbb{E}_{\hat{\theta}_0, \hat{\theta}_1}[\tilde{Y}_{\text{val}} \mid X = x] &= \sum_{y_0 \in \mathcal{F}(x), y_1 \in \mathcal{F}(x)} \mathbb{P}[\hat{Y}_0 = y_0, \hat{Y}_1 = y_1] \mathbb{E}_{\hat{\theta}_0, \hat{\theta}_1}[\tilde{Y}_{\text{val}} \mid X = x, \hat{Y}_0 = y_0, \hat{Y}_1 = y_1] \\
&= \sum_{y_0 \in \mathcal{F}(x), y_1 \in \mathcal{F}(x)} \mathbb{P}[\hat{Y}_0 = y_0, \hat{Y}_1 = y_1] \mathbb{E}_{\hat{\theta}_0, \hat{\theta}_1}[\tilde{Y}_{\text{val}} \mid X = x, \hat{\theta}_0 \in \Phi_x(y_0), \hat{\theta}_1 \in \Phi_x(y_1)] \\
&= \sum_{y_0 \in \mathcal{F}(x), y_1 \in \mathcal{F}(x)} \mathbb{P}[\hat{Y}_0 = y_0, \hat{Y}_1 = y_1] \mathbb{E}_{\hat{\theta}_0, \hat{\theta}_1}[\tilde{Y}_{\text{val}} \mid X = x, \hat{\theta}_0 \in \Phi_x(y_0), \hat{\theta}_1 \in \Phi_x(y_1)]
\end{aligned} \tag{20}$$

$$\begin{aligned}
& \mathbb{E}_{\hat{\theta}_0, \hat{\theta}_1} [\tilde{Y}_{\text{val}} | X = x, \hat{\theta}_0 \in \Phi_x(y_0), \hat{\theta}_1 \in \Phi_x(y_1)] \\
&= \mathbb{E}_{\hat{\theta}_0, \hat{\theta}_1} [(1 - Z)y_0 + Zy_1 | X = x, \hat{\theta}_0 \in \Phi_x(y_0), \hat{\theta}_1 \in \Phi_x(y_1)] \\
&= \mathbb{P}[h_{\text{val}}(\hat{\theta}_0, x) < h_{\text{val}}(\hat{\theta}_1, x) | X = x, \hat{\theta}_0 \in \Phi_x(y_0), \hat{\theta}_1 \in \Phi_x(y_1)]y_0 + \\
& \quad \mathbb{P}[h_{\text{val}}(\hat{\theta}_0, x) > h_{\text{val}}(\hat{\theta}_1, x) | X = x, \hat{\theta}_0 \in \Phi_x(y_0), \hat{\theta}_1 \in \Phi_x(y_1)]y_1
\end{aligned} \tag{21}$$

Without loss of generality say $y_0 < y_1$

$$\begin{aligned}
& \mathbb{P}\left[h_{\text{val}}(\hat{\theta}_0, x) < h_{\text{val}}(\hat{\theta}_1, x) | X = x, \hat{\theta}_0 \in \Phi_x(y_0), \hat{\theta}_1 \in \Phi_x(y_1)\right] > \\
& \mathbb{P}\left[|h_{\text{val}}(\hat{\theta}_0, x) - y_0| < \frac{\Delta}{2}, |h_{\text{val}}(\hat{\theta}_1, x) - y_1| < \frac{\Delta}{2} \mid X = x, \hat{\theta}_0 \in \Phi_x(y_0), \hat{\theta}_1 \in \Phi_x(y_1)\right]
\end{aligned} \tag{22}$$

$h_{\text{val}}(\hat{\theta}_0, x)$ and $h_{\text{val}}(\hat{\theta}_1, x)$ are both conditionally independent given $\hat{\theta}_0 \in \Phi_x(y_0), \hat{\theta}_1 \in \Phi_x(y_1)$ (can be observed by decomposing the joint distributions). As a result, we can simplify the above expression as follows.

$$\begin{aligned}
& \mathbb{P}\left[|h_{\text{val}}(\hat{\theta}_0, x) - y_0| < \frac{\Delta}{2}, |h_{\text{val}}(\hat{\theta}_1, x) - y_1| < \frac{\Delta}{2} \mid X = x, \hat{\theta}_0 \in \Phi_x(y_0), \hat{\theta}_1 \in \Phi_x(y_1)\right] \\
& \mathbb{P}\left[|h_{\text{val}}(\hat{\theta}_0, x) - y_0| < \frac{\Delta}{2} \mid X = x, \hat{\theta}_0 \in \Phi_x(y_0)\right] \mathbb{P}\left[|h_{\text{val}}(\hat{\theta}_1, x) - y_1| < \frac{\Delta}{2} \mid X = x, \hat{\theta}_1 \in \Phi_x(y_1)\right] \\
&= \left(1 - \frac{\epsilon}{2f^{\text{sup}}}\right)^2 > 1 - \frac{\epsilon}{f^{\text{sup}}}
\end{aligned} \tag{23}$$

Therefore, when $y_0 < y_1$ we get

$$\mathbb{E}_{\hat{\theta}_0, \hat{\theta}_1} [\tilde{Y}_{\text{val}} | X = x, \hat{\theta}_0 \in \Phi_x(y_0), \hat{\theta}_1 \in \Phi_x(y_1)] \leq \left(1 - \frac{\epsilon}{f^{\text{sup}}}\right)y_0 + \frac{\epsilon}{f^{\text{sup}}}y_1 \tag{24}$$

In general we can write

$$\begin{aligned}
\mathbb{E}_{\hat{\theta}_0, \hat{\theta}_1} [\tilde{Y}_{\text{val}} | X = x, \hat{\theta}_0 \in \Phi_x(y_0), \hat{\theta}_1 \in \Phi_x(y_1)] &\leq \left(1 - \frac{\epsilon}{f^{\text{sup}}}\right) \min\{y_0, y_1\} + \frac{\epsilon}{f^{\text{sup}}} \max\{y_0, y_1\} \\
&\leq \min\{y_0, y_1\} + \epsilon
\end{aligned} \tag{25}$$

Substituting (25) in (20) to obtain

$$\mathbb{E}_{\{\hat{\theta}_k\}_{k=0}^{M-1}} [\tilde{Y}_{\text{val}} | X = x] \leq \mathbb{E}_{\{\hat{\theta}_k\}_{k=0}^{M-1}} \left[\min_{k \in \{1, \dots, M\}} \{\hat{Y}_k\} | X = x \right] + \epsilon \tag{26}$$

□

We restate Proposition 6 below.

Proposition 12. *If Assumption 5 holds and the prediction error of h_{arg} is small, i.e. $0 < s < 1$, $0 < \eta < 1$, $\mathbb{E}_{X, \hat{\theta}} [\|h_{\text{arg}}(\hat{\theta}, X) - g^\dagger(\hat{\theta}, X)\|^2] \leq s(1 - \epsilon)(\delta\eta)^2$, where ϵ, δ are from Assumption 5, then with probability $(1 - s)(1 - \epsilon)$ Arg-Init achieves η -factor reduction.*

Proof. Consider the event

$$\|h_{\text{arg}}(\hat{\theta}, X) - g^\dagger(\hat{\theta}, X)\|^2 < (\delta\eta)^2$$

and $\hat{\theta} \notin B_\delta$, i.e.

$$\|\hat{\theta} - g^\dagger(\hat{\theta}, X)\|^2 \geq (\delta)^2$$

The above event is equivalent to saying that the initializer from $\hat{\theta}$ starts at a larger distance (a factor η larger) from the true solution than the one found by the learned model.

We use Markov's inequality on the complement of the first event above as follows

$$\mathbb{P}_{\hat{\theta}, X} \left[\|h_{\text{arg}}(\hat{\theta}, X) - g^\dagger(\hat{\theta}, X)\|^2 \geq (\delta\eta)^2 \mid \hat{\theta} \notin B_\delta \right] \leq \frac{\mathbb{E}_{\hat{\theta}, X} \left[\|h_{\text{arg}}(\hat{\theta}, X) - g^\dagger(\hat{\theta}, X)\|^2 \mid \hat{\theta} \notin B_\delta \right]}{(\delta\eta)^2} \quad (27)$$

Next we use Assumption 5 to get a bound on

$$\mathbb{E}_{\hat{\theta}, X} \left[\|h_{\text{arg}}(\hat{\theta}, X) - g^\dagger(\hat{\theta}, X)\|^2 \mid \hat{\theta} \notin B_\delta \right]$$

as follows

$$\begin{aligned} & \mathbb{E}_{\hat{\theta}, X} \left[\|h_{\text{arg}}(\hat{\theta}, X) - g^\dagger(\hat{\theta}, X)\|^2 \right] \\ &= \mathbb{E}_{\hat{\theta}, X} \left[\|h_{\text{arg}}(\hat{\theta}, X) - g^\dagger(\hat{\theta}, X)\|^2 \mid \hat{\theta} \notin B_\delta \right] \times \mathbb{P}[\hat{\theta} \notin B_\delta] + \\ & \quad (1 - \mathbb{P}[\hat{\theta} \notin B_\delta]) \mathbb{E}_{\hat{\theta}, X} \left[\|h_{\text{arg}}(\hat{\theta}, X) - g^\dagger(\hat{\theta}, X)\|^2 \mid \hat{\theta} \in B_\delta \right] \\ & \implies \mathbb{E}_{\hat{\theta}, X} \left[\|h_{\text{arg}}(\hat{\theta}, X) - g^\dagger(\hat{\theta}, X)\|^2 \mid \hat{\theta} \notin B_\delta \right] \leq 1/(1 - \epsilon) \mathbb{E}_{\hat{\theta}, X} \left[\|h_{\text{arg}}(\hat{\theta}, X) - g^\dagger(\hat{\theta}, X)\|^2 \right] \end{aligned} \quad (28)$$

Using the above equation (27) in the RHS in Markov inequality (28)

$$\mathbb{P} \left[\|h_{\text{arg}}(\hat{\theta}, X) - g^\dagger(\hat{\theta}, X)\|^2 \geq (\delta\eta)^2 \mid \hat{\theta} \notin B_\delta \right] \leq \frac{\mathbb{E}_{\hat{\theta}, X} \left[\|h_{\text{arg}}(\hat{\theta}, X) - g^\dagger(\hat{\theta}, X)\|^2 \right]}{(1 - \epsilon)(\delta\eta)^2} \quad (29)$$

Substitute the condition on the prediction error stated in the statement of the Proposition to get

$$\mathbb{P} \left[\|h_{\text{arg}}(\hat{\theta}, X) - g^\dagger(\hat{\theta}, X)\|^2 \geq (\delta\eta)^2 \mid \hat{\theta} \notin B_\delta \right] \leq s \quad (30)$$

We simplify the probability of the event defined (the event leads to η -factor reduction) in the beginning of the proof as

$$\begin{aligned} & \mathbb{P} \left[\|h_{\text{arg}}(\hat{\theta}, X) - g^\dagger(\hat{\theta}, X)\|^2 \leq (\delta\eta)^2, \hat{\theta} \notin B_\delta \right] \\ &= \mathbb{P} \left[\|h_{\text{arg}}(\hat{\theta}, X) - g^\dagger(\hat{\theta}, X)\|^2 \leq (\delta\eta)^2 \mid \hat{\theta} \notin B_\delta \right] \times \mathbb{P}[\hat{\theta} \notin B_\delta] \\ &\geq \mathbb{P} \left[\|h_{\text{arg}}(\hat{\theta}, X) - g^\dagger(\hat{\theta}, X)\|^2 \leq (\delta\eta)^2 \mid \hat{\theta} \notin B_\delta \right] (1 - \epsilon) \end{aligned} \quad (31)$$

We substitute equation (30) in (31) equation to obtain

$$\mathbb{P}\left[\|h_{\text{arg}}(\hat{\theta}, X) - g^\dagger(\hat{\theta}, X)\|^2 \leq (\delta\eta)^2 \cap \hat{\theta} \notin B_\delta\right] \geq (1-s)(1-\epsilon) \quad (32)$$

This completes the proof. \square

6.2 Connection between Proposition 3 and uniform random binary classifier

In Proposition 3, we show that correlation between model's probabilities and the label is positive, then the model is better at initialization than a random classifier. In standard binary classification problems as well, a similar result exists, i.e., if the classifier's output is positively correlated with the label, then it performs better than uniform random classification. We derive his result next for completeness.

We are given labeled data with labels $Y \in \{1, -1\}$. Suppose the two classes occur with equal probability then $\mathbb{E}[Y] = 0$. Define the output of the classifier as $P \in \{1, -1\}$.

Define $A = \frac{1+YP}{2}$. If $Y = 1, P = 1$ or $Y = -1, P = -1$, then $A = 1$. If $Y = 1, P = -1$ or $Y = -1, P = 1$, then $A = 0$. Observe that $\mathbb{E}[A]$ is the accuracy of the classifier P . Let us simplify $\mathbb{E}[YP]$. $\mathbb{E}[YP] = \mathbb{E}[Y]\mathbb{E}[P] + \rho(Y, P)\sigma_Y\sigma_P$, where $\rho(Y, P)$ is the correlation between Y and P , σ_Y and σ_P are the standard deviation of Y and P .

Simplify

$$\mathbb{E}[A] = \frac{1 + \mathbb{E}[YP]}{2} = \frac{1 + \rho(Y, P)\sigma_Y\sigma_P}{2}$$

If the correlation is positive $\rho(Y, P) > 0$, the accuracy is greater than $\frac{1}{2}$. A uniform random binary classifier has an accuracy of $\frac{1}{2}$. If correlation is negative $\rho(Y, P) < 0$, then accuracy is less than $\frac{1}{2}$ but can be made greater than $\frac{1}{2}$ by flipping the sign of the output of P .

6.3 Correlation between m and $\hat{Y}_1 - \hat{Y}_0$

Below Proposition 3, we stated that it is reasonable to expect a positive correlation between m and $\hat{Y}_1 - \hat{Y}_0$. m is trained to predict $\hat{Y}_1 - \hat{Y}_0$. For simplicity let us call $\hat{Y}_{\text{diff}} = \hat{Y}_1 - \hat{Y}_0$. Suppose the loss function used to train m is mean squared error $\mathbb{E}[(\hat{Y}_{\text{diff}} - m(X, \hat{\theta}_0, \hat{\theta}_1))^2]$.

$$\begin{aligned} \mathbb{E}[(\hat{Y}_{\text{diff}} - m(X, \hat{\theta}_0, \hat{\theta}_1))^2] &= \mathbb{E}[(\hat{Y}_{\text{diff}})^2] + \mathbb{E}[(m(X, \hat{\theta}_0, \hat{\theta}_1))^2] - 2\mathbb{E}[\hat{Y}_{\text{diff}}(m(X, \hat{\theta}_0, \hat{\theta}_1))] \\ &= \mathbb{E}[(\hat{Y}_{\text{diff}})^2] + \mathbb{E}[(m(X, \hat{\theta}_0, \hat{\theta}_1))^2] - 2\rho(Y_{\text{diff}}, m)\sigma_{Y_{\text{diff}}}\sigma_{m(X, \hat{\theta}_0, \hat{\theta}_1)} \end{aligned}$$

Consider we are given a function $m'(X, \hat{\theta}_0, \hat{\theta}_1)$. Our task is to learn a function m , which is a scalar multiple of m' defined as $m(X, \hat{\theta}_0, \hat{\theta}_1) = am'(X, \hat{\theta}_0, \hat{\theta}_1)$, such that it minimizes the loss defined above.

Suppose $\rho(Y_{\text{diff}}, m')$ is the correlation between m' and \hat{Y}_{diff} . If $\rho(Y_{\text{diff}}, m') = 0$, then the optimal $a = 0$. If $\rho(Y_{\text{diff}}, m') > 0$, then the optimal $a > 0$ and thus $\rho(Y_{\text{diff}}, m) > 0$. If $\rho(Y_{\text{diff}}, m') < 0$, then the optimal $a < 0$ and thus $\rho(Y_{\text{diff}}, m) > 0$. Therefore, if $\rho(Y_{\text{diff}}, m') \neq 0$, then the $\rho(Y_{\text{diff}}, m) > 0$ and if $\rho(Y_{\text{diff}}, m') = 0$, then optimal model $m = 0$. As long as any learning happens, i.e. a non-zero model m is learned it has a finite and positive correlation with Y_{diff} . The condition in Corollary 1 requires $\frac{e^m}{1+e^m}$ to be positively correlated with Y_{diff} . [Egozcue et al., 2009] establishes sufficient conditions (Y_{diff} and $m(X, \hat{\theta}_0, \hat{\theta}_1)$ have positive quadrant dependency) under which even under simple transformations of a variable the sign of the correlation is preserved.

7 Supplement to Experiments

The experiments were conducted on 2.3 GHz Intel Core i9 with 32 GB RAM (2400 MHz and DDR4). We used keras to train all the models. For any hyperparameter that we do not specify, we use the default values (for e.g., initializer for NN is set to Glorot uniform). We organize this section as follows. There are five problem families that we work with – a) convex optimization (minimize linear form of the problem in equation (2)), b) Ackley function minimization, c) generating adversarial examples, d) generating contrastive explanations, e) sum-rate optimization. We start by describing the datasets and the models for which we generate adversarial examples and contrastive explanations. After that we describe the different initializers that were used, which is followed by the description of the gradient descent solvers for each of the problems. Lastly, we provide the supplementary experiments results.

7.1 Datasets and Models for Adversarial Examples and Contrastive Explanations

CIFAR-10 dataset and model. The data can be downloaded from ¹. We use the default train-test split. We train a multi-layer convolutional neural network. The first layer uses 32 convolutional filters, with kernel size (3, 3) and ReLU activation. It is followed by a maxpool layer. The third layer uses 64 convolutional filters, with kernel size (3, 3) and ReLU activation. It is followed by a maxpool layer. The last layer flattens the output from third layer, outputs softmax scores for the 10 classes onto the 10 output nodes. The model is then trained using cross-entropy loss function with Adam optimizer. We use a learning rate of 1e-3. The total number of training epochs were set to 10. The trained model achieves 70 percent test accuracy.

MNIST digits dataset The data can be downloaded from ². We use the standard split in MNIST digits. We use a two layer neural network, where the first layer (the hidden layer) has 128 nodes with ReLU activation, and the second layer (the output layer) has 10 output nodes with softmax activation. The model is trained using cross-entropy loss function with Adam optimizer. We set a learning rate of 1e-3 and the other parameters of Adam are set to default value. The total number of training epochs were set to 10. The trained model achieves 97 percent accuracy.

HELOC dataset and model. The dataset can be downloaded from ³. Home equity line of credit (HELOC) data contains the information about the applicant in their credit report and their loan repayment history. We build a model to predict whether applicants will make timely payments. We divided the data into 75 percent train, 25 percent test. We use a two layer neural network, where the first layer (the hidden layer) has 200 nodes with ReLU activation and the second layer (the output layer) has two output nodes with softmax activation. The model is trained using cross-entropy loss function with Adam optimizer. We set a learning rate of 1e-3 and the other parameters of Adam are set to default value. The total number of training epochs were set to 20. The trained model achieves 72 percent accuracy.

Waveform dataset The dataset can be downloaded from ⁴. The dataset consists of 40 attributes that help identify the wave type (from three types of waves). We divided the data into 75 percent train, 25 percent test. We use a two layer neural network, where the first layer (the hidden layer) has

¹<https://www.cs.toronto.edu/~kriz/cifar.html>

²https://www.tensorflow.org/api_docs/python/tf/keras/datasets/mnist

³<https://community.fico.com/s/explainable-machine-learning-challenge?tabset-3158a=2>

⁴<https://archive.ics.uci.edu/ml/machine-learning-databases/waveform/>

200 nodes with ReLU activation and the second layer (the output layer) has three output nodes with softmax activation. The model is trained using cross-entropy loss function with Adam optimizer. We set a learning rate of 1e-3 and the other parameters of Adam are set to default value. The total number of training epochs were set to 20. The trained model achieves 85 percent accuracy.

7.2 Initializers

We discuss the different initializers. Each of these initializers pick a value for θ_{in} for gradient descent solver in the Algorithm 1.

Zero initializer. This is the simplest of the benchmarks. We start gradient descent with zero vector as initialization. Note that when using it for adversarial examples, and the contrastive explanations, we use the loss function in [Cheng et al., 2018] whose gradient involves $\frac{\theta}{\|\theta\|}$, where θ is the perturbation. This term undefined at zero, which is why we add a very small noise term to zero vector to avoid undefined gradient values.

Random initializer. In this benchmark, we have to choose a distribution from which we sample the random initializations. For convex optimization, we initialize the optimization variable θ in equation (2) is drawn from standard uniform distribution (each component of the optimization variable is sampled from a uniform distribution over $[0, 1]$). For the two dimensional Ackley function minimization defined in the main body of the paper, we use a uniform random initializer over the set $[-5, 5] \times [-5, 5]$. For contrastive explanations and adversarial examples on tabular datasets, we draw an initialization from standard uniform distribution (the dimension of the initializer is the same as the dimensionality of the dataset). For contrastive explanations and adversarial examples on MNIST digits data, we found that standard uniform random did not perform well. Instead, we found that sampling points from the training dataset itself worked better. For these settings we used uniform sampling over the training data set. For sum-rate optimization problem, each component of the optimization variable is sampled from a uniform distribution over $[0, 1]$

MAML initializer. In [Finn et al., 2017], MAML was proposed for learning models that perform well on few-shot learning tasks. MAML procedure can be understood as a way of generating an effective initialization for a model which quickly adapts to new tasks. The steps in MAML initialization applied to the optimization problem in equation (1) are given in Algorithm 3. The output of the algorithm is the initialization vector we use to solve the problem for new instances. For the different methods, we use a batch size $K = 32$ for MAML initializer, $\alpha = 0.01$, and $\beta = 0.01/K$, where α and β are the learning rates in the Algorithm 3.

Val-Init Initializer. Recall Val-Init Algorithm (described in the main body of the paper) has two phases. In the first phase, we use random initializer (described above) and solve the problem to generate training data for the next phase. We learn a model from a hypothesis class \mathcal{H}_{val} , which we define next. The model for Val-Init is a 3 layer neural network. The shape of the input layer depends on the problem (for generating adversarial examples and contrastive explanations the size of the layer is $2 * \text{input-shape}$, where input-shape is the dimension of each data instance). The two hidden layers have 200 nodes and ReLU activations. The output layer has one node. The model is trained using mean squared error loss function with Adam optimizer. We set a learning rate of 1e-3 and the other parameters of Adam are set to default value. The total number of training epochs were set to 100.

Arg-Init Initializer. Recall Arg-Init Algorithm (described in the main body of the paper) has two phases. In the first phase, we use random initializer (the choice of random initializer was already described above) and solve the problem to generate training data for the next phase. We learn

Algorithm 3 MAML Initializer

Input: Instances $\{X_i\}_{i=0}^\infty$
 Π_Θ : projection on the set Θ
 $\theta \leftarrow$ random initialize
for $i \in \{0, \dots, N-1\}$ **do**
 Sample a batch of size K of optimization tasks $\{X_t\}_{t=1}^K \in \mathbb{P}_X$
 for $t \in \{1, \dots, K\}$ **do**
 Update $\theta_t = \Pi_\Theta(\theta - \alpha \nabla_\theta f(\theta, X_t))$
 end for
 $\theta = \Pi_\Theta(\theta - \beta \sum_{t=1}^K \nabla_\theta f(\theta_t, X_t))$
end for
Output: θ

a model from a hypothesis class \mathcal{H}_{arg} , which we define next. The model for Arg-Init is a 3 layer neural network. The shape of the input layer depends on the problem (for generating adversarial examples and contrastive explanations the size of the layer is $2 * \text{input-shape}$, where input-shape is the dimension of each data instance). The two hidden layers have 200 nodes and ReLU activations. The output layer has the same number of dimensions as the dimension of each data instance. The model is trained using mean squared error loss function with Adam optimizer. We set a learning rate of 1e-3 and the other parameters of Adam are set to default value. The total number of training epochs were set to 100.

Remark about h_{val} and h_{arg} CIFAR-10. When learning h_{val} and h_{arg} for CIFAR-10 dataset, we do not feed raw images to the network of the three layer MLPs described above. Instead, we first extract the representation of these images from the convolutional neural network model (described in Section 7.1) trained to predict the labels in CIFAR-10. We extract these representations from the layer before the output layer.

7.3 Solvers and other details

In all the problems, we use gradient descent based solvers described in Algorithm 3 in the main body of the paper. The gradient descent solver in Algorithm 1 is supplied an input of step update rules to use, and we for our experiments use– in iteration k take a step length $\frac{p}{q+k}$

Convex optimization setting. Consider the problem in equation (2), we set $\beta = 1$. We set u to be a linear classifier $u(x) = a^t x$, where $a \in \mathbb{R}^m$ and $x \in \mathbb{R}^m$ are the parameters that are fixed for an instance of the optimization. We run experiments for $m = 50, 75, 100$. We keep the classifier a fixed (a random normal vector) and vary the input example x across problem instances (each new instance x is also a random normal vector). Our goal is to solve for the optimal perturbation θ . We use projected subgradient descent (PGD) based approach to solve this problem. The projection part is needed to ensure constraints are exactly satisfied. We use subgradients as the loss function involves an ℓ_1 norm term. We set $p = 1$ and $q = 25$ in the step update rule.

For training Val-Init and Arg-Init, we need to generate training data (See Algorithm 2 in the main body of the paper). We use a random initializer (described in Section 7.2) in the first phase of the algorithm. The number of examples for which we solve the problem in Phase 1 of the Algorithm 2, N is set to 1500. In the second phase, we test on 500 instances.

Ackley function minimization. Ackley functions are used to study non-convex optimization

problems [Ackley, 2012]. The general form of a two dimensional Ackley function is

$$A(x, y, a, b, c) = -a \exp\left(-b \frac{\sqrt{(x-c)^2 + (y-c)^2}}{2}\right) - \exp\left(\frac{\cos(2\pi(x-c)) + \cos(2\pi(y-c))}{2}\right) + \exp(1) + a \quad (33)$$

The global minimum of the function is at (c, c) and the minimum value is zero. We are given a sequence of functions with different values of a, b, c , where $a \sim 20 + U[0, 10]$, $b \sim 0.2 + U[0, 0.1]$ and $c \sim U[0, 2]$ and our goal is to learn an initializer that takes a, b, c as input and generates an initialization. We set $p = 0.25$ and $q = 1$ in the step update rule. For training Val-Init and Arg-Init, we need to generate data in the first phase. We use a random initializer as described in the previous section. The number of examples for which we solve the problem in Phase 1 of the Algorithm 2, N is set to 1500. In the second phase, we test on 500 instances.

Adversarial examples. Consider the problem in equation (2) in the main body of the paper, we set $\beta = 0$. We set u to be a neural network model that we learn for the specific dataset (CIFAR-10, HELOC, MNIST, Waveform). As we explained in the manuscript, we use a penalty based version of the problem in equation (2) in the main body (following the approach in [Cheng et al., 2018]). We set the value of the margin, which is a parameter in the penalty term, to be 0.2. We set the penalty value such that the fraction of constraints satisfied in equation (2) by random initialization is high. Hence, the penalty value varies across datasets. For MNIST digits the penalty value is set to be 2.5. For HELOC and Waveform datasets the penalty value is set to be 10. For CIFAR-10 dataset the penalty value is set to be 50. We use a standard gradient descent based solver as the objective is differentiable. For CIFAR-10, MNIST digits we set the step update parameters as follows $p = 1$, $q = 1$. For tabular datasets (HELOC, Waveform) we set the step update parameters as follows $p = 1$, $q = 5$. Recall we described the split of HELOC, Waveform and MNIST data into train and test, which were used to learn models (Section 7.1). We use the same training data to generate the adversarial examples (Phase 1 of the Algorithm 2 in the main body) and use the same testing data to compare the different initializers.

Contrastive explanations. Consider the problem in equation (2) in the main body, we set $\beta = 0.1$ and constrain the perturbations to be valid contrastive explanations (as described in [Dhurandhar et al., 2018]). We set u to be a neural network model that we learn for the specific dataset (MNIST, Waveform). We consider a penalty based version of the problem in equation (2) in the main body (following the approach in [Dhurandhar et al., 2018]). We use the same values for the margin and penalties as in the case for adversarial examples. We use subgradient descent based solver (as described in [Dhurandhar et al., 2018]). For MNIST digits we set the step update parameters as follows $p = 1$, $q = 1$. For tabular datasets (HELOC, Waveform) we set the step update parameters as follows $p = 1$, $q = 5$. Recall we described the split of HELOC, Waveform and MNIST data into train and test, which were used to learn models (Section 7.1). We use the same training data to generate the contrastive explanations (Phase 1 of the Algorithm 2 in the main body) and use the same testing data to compare the different initializers.

Sum-rate optimization. We use projected gradient descent based solver, where projections are on the set of constraints of the optimization problem, i.e., $[0, 1]^m$. We set the step update parameters as $p = 1$, $q = 1$. For sum-rate optimization, we train using 5000 problem instances for 15 users. Each problem instance is a new independent draw of the channel matrix from a standard uniform random distribution (each element in the matrix is i.i.d.). We learn initializations for Val-Init, Arg-Init, and MAML. We test on the 500 instances.

Please note that we did not specify the number of iterations that we fix in gradient descent because we show a comparison of the performance with varying number of iterations in the solver.

7.4 Results

7.4.1 Convex optimization experiments

We compare the methods in terms of the average value of the objective function across the test instances (the best method should have the smallest value) for the same number of iterations. In Figure 6, we plot the objective function value achieved by the different approaches vs. the number of iterations when $m = 75$. Arg-Init is able to find a much better solution (35-70% reduction) when the number of iterations are small. When the iterations increase all the methods perform well (since the problem is convex) and the method eventually finds the minimum. In Figure 7, we present the distribution of the objective function values for the different methods for $m = 75$. Observe that Arg-Init’s distribution is skewed towards the left and its performance stochastically dominates the other methods. We also present results for additional cases here for $m = 50$ and $m = 100$. See the results in Table 3, where we show Arg-Init continues to beat other methods. In addition to the comparisons, we provide validation mean square error values for learners h_{val} , h_{arg} to show that these methods models were able to learn based on the instances supplied to them at the end of Phase 1 of Algorithm 1 in the main body. In Table 4, we provide initial and final validation mean square error values.

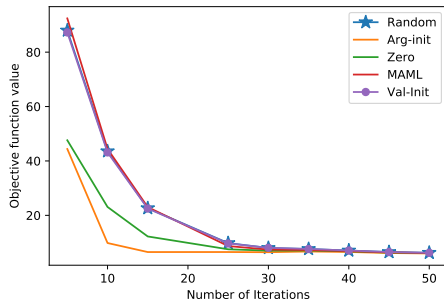


Figure 6: Objective fun vs. number of iterations

Table 3: **Convex optimization setting:** Objective’s average value, fraction of instances when constraints not satisfied and the number of iterations per instance in test phase.

METHOD	$m = 50$	$m = 75$	$m = 100$
RANDOM	29.69, 0.0, 10	43.56, 0.0, 10	57.68, 0.0, 10
ZERO	16.07, 0.0, 10	23.08, 0.0, 10	29.75, 0.0, 10
MAML	29.84, 0.0, 10	44.43, 0.0, 10	59.51, 0.0, 10
ARG-INIT	7.70, 0.0, 10	9.82, 0.0, 10	12.75, 0.0, 10
VAL-INIT	28.95, 0.0, 10	43.14, 0.0, 10	57.18, 0.0, 10

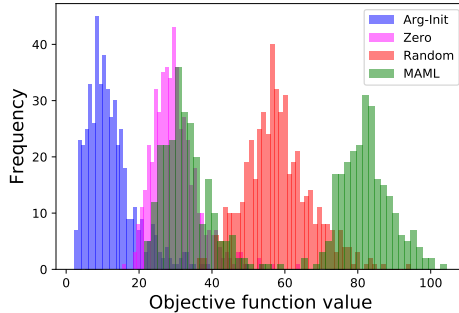


Figure 7: Convex optimization setting: Histogram comparing the objective function value distribution

Table 4: **Convex optimization setting:** Learner errors h_{val} (h_{arg})

METHOD	$m = 50$	$m = 75$	$m = 100$
EPOCH 1 (FIRST)	9.22 (0.026)	13.34 (0.0020)	33.06 (0.0015)
EPOCH 100 (LAST)	0.11 (0.010)	0.24 (0.0004)	0.02 (0.0005)

7.4.2 Ackley function minimization

In the main body, we presented the experiments for Ackley function minimization: objective function value vs number of iterations. Here we provide the plot of distribution of the objective function values (when number of iterations are fixed to 50). In Figure 8, we observe that the scores of Val-Init lie most to the left. Since the distributions are very skewed, we provide a Zoomed in view in Figure 9. We also provide the validation mean square error when learning h_{val} and h_{arg} . The initial (epoch 1) and final (epoch 100) mean square error values for h_{val} (h_{arg}) are 18.48 (1.46) and 5.52 (0.10), which reflect these models can learn their respective labels well.

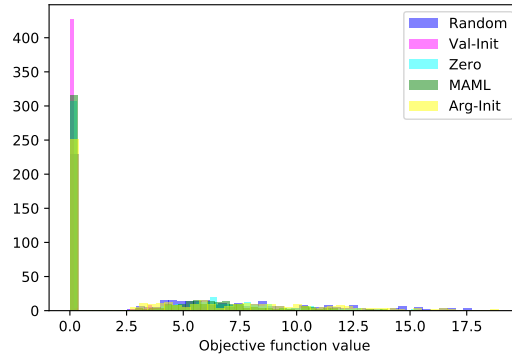


Figure 8: Ackley function minimization: Histogram comparing the objective function value distribution.

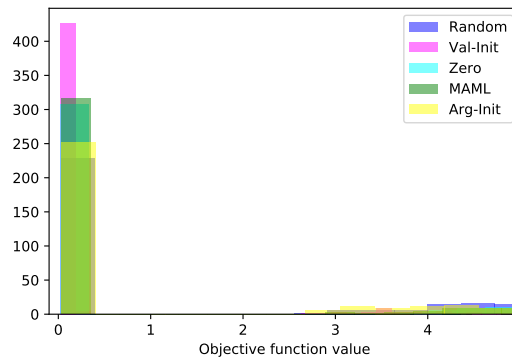


Figure 9: Ackley function minimization: Histogram comparing the objective function value distribution (Zoomed in version).

7.4.3 Generating adversarial examples

CIFAR-10 dataset. In the main body, we presented the experiments for CIFAR-10 dataset: performance of the method vs. number of iterations. We provide additional details on this comparison below. In Figure 10, we provide a histogram of distribution of performance values of the methods over different problem instances (for the case when number of iterations is set to 100). Both Val-Init and Arg-Init have a consistently good performance over all instances (as their distributions towards the left) unlike zero initializer which has an erratic performance distribution – in some instances it can successfully generate good initializers while in others it is far off.

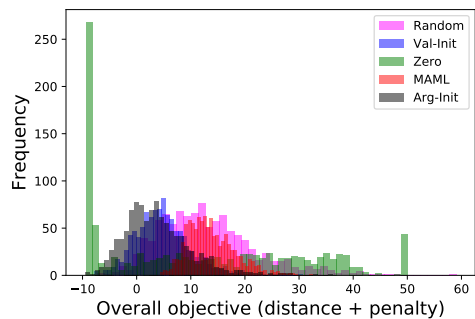


Figure 10: CIFAR-10: Histogram of objective values for Arg-Init, Random, Zero, MAML initialization

MNIST Digits. In the main body in Table 1, we showed the average performance of the different initializers on MNIST. In Figure 11, we present the histogram comparing the distribution of performance over the different instances. Since the comparison in Table 1 in the main body is for a fixed number of iterations, in Figure 12, we present the plot the performance of the method vs. the number of iterations. We also provide the validation mean square error when learning h_{val} and h_{arg} . For Arg-Init (Val-Init) the MSE at the end of first epoch: 0.0089 (0.79) and at the end of last epoch: 0.0026 (0.33).

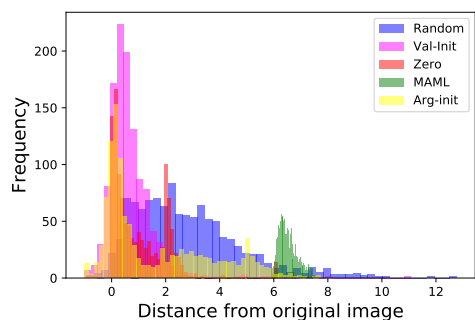


Figure 11: Adversarial example MNIST digits: Histogram comparing the distribution of the average penalized objective.

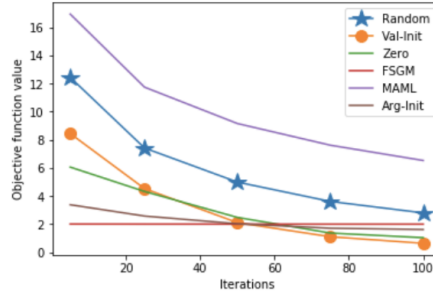


Figure 12: Adversarial example MNIST digits: Compare performance (average penalized objective function value across test instances) of the method vs. iterations for Val-Init, Arg-Init, Random, Zero, MAML initialization.

Waveform dataset. In the main body in Table 1, we showed the average performance of the different initializers on Waveform and found Arg-Init, Zero and MAML were very close. In Figure 13, we show the distribution of the performance of the methods over the different instances. Arg-Init, Zero and MAML lie on the left most side of the histogram, while Val-Init and Random are on the right side. In Figure 14, we compare the performance of the methods for different number of iterations and we find that MAML performs the best and as number of iterations increase Arg-Init closes in on MAML’s performance. We also provide the validation mean square error when learning h_{val} and h_{arg} . The initial (epoch 1) and final (epoch 100) mean square error values for h_{val} (h_{arg}) are 0.0296 (0.0047) and 0.0233 (0.0008), which reflect these models can learn their respective labels well.

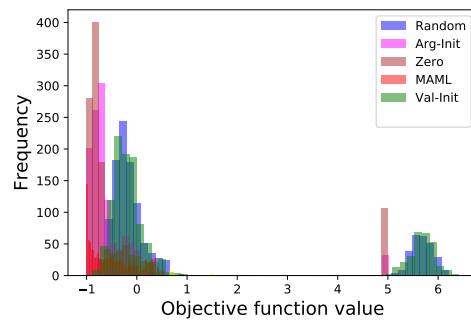


Figure 13: Adversarial example waveform data: Histogram of performance of methods Val-Init, Arg-Init, Random, Zero, MAML initialization

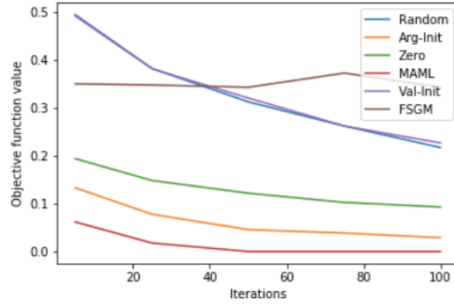


Figure 14: Adversarial example waveform data: Compare the distance from the original point vs iterations for Val-Init, Arg-Init, Random, Zero, MAML initialization

HELOC dataset. In the main body in Table 1, we showed the average performance of the different initializers for a fixed number of iterations. In Figure 15, we compare the different methods in terms of performance of methods vs. the number of iterations. We also provide the validation mean square error when learning h_{val} and h_{arg} . The initial (epoch 1) and final (epoch 100) mean square error values for h_{val} (h_{arg}) are 0.0369 (0.0046) and 0.0152 (0.0007), which reflect these models can learn their respective labels well.

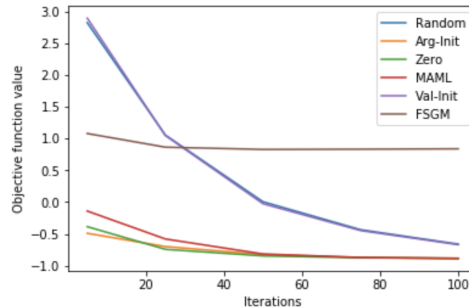


Figure 15: Adversarial example HELOC data: Compare the distance from the original point vs. iterations for Val-Init, Arg-Init, Random, Zero, MAML initialization

7.5 Contrastive Explanations

7.5.1 MNIST Digits

In the main body, we presented the comparison for MNIST digits for a fixed number of iterations. In the main body in Table 2, we showed the average performance of the different initializers on MNIST. In Figure 16, we present the histogram comparing the distribution of performance over the different instances. Observe that Arg-Init is the most towards the left. Since the comparison in Table 2 in the main body is for a fixed number of iterations, in Figure 17, we present the plot the performance of the method vs. the number of iterations. We also provide the validation mean square error when

learning h_{val} and h_{arg} . For Arg-Init (Val-Init) the MSE at the end of first epoch: 0.0175 (0.097) and at the end of last epoch: 0.0071 (0.057).

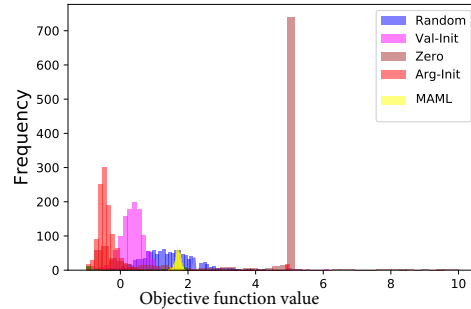


Figure 16: Contrastive explanations MNIST digits: Compare the distance from the original point vs iterations for Val-Init, Arg-Init, Random, Zero, MAML initialization.

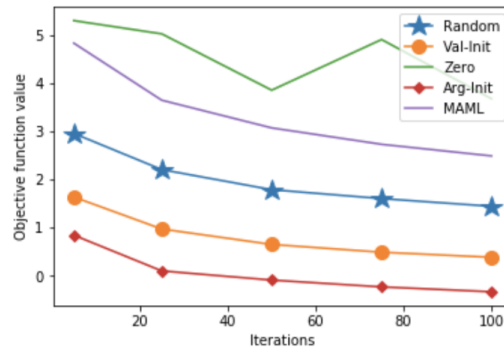


Figure 17: Contrastive explanations MNIST digits: Compare the performance of method vs iterations for Val-Init, Arg-Init, Random, Zero, MAML initialization.

7.5.2 Waveform dataset

In the main body in Table 2, we showed the average performance of the different initializers. In Figure 18, we compare the histogram of distance from the original point (for iterations fixed to 100). Arg-Init is the most skewed towards the left compared to the other distributions. In Figure 19, we compare the objective function value vs. the iterations. We also provide the validation mean square error when learning h_{val} and h_{arg} . For Arg-Init (Val-Init) the MSE at the end of first epoch: 0.027 (6.99) and at the end of last epoch: 0.0076 (2.69).

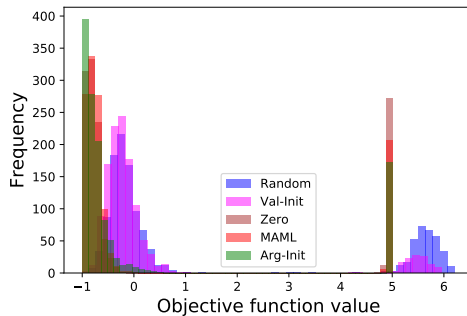


Figure 18: Contrastive explanations Waveform dataset: Compare the performance of method vs iterations for Val-Init, Arg-Init, Random, Zero, MAML initialization.

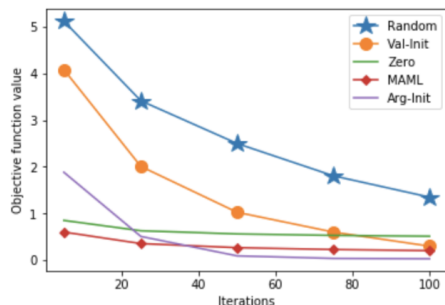


Figure 19: Contrastive explanations Waveform dataset: Compare the performance of method vs iterations for Val-Init, Arg-Init, Random, Zero, MAML initialization.

7.5.3 Sum-rate optimization

In the main body we showed how for sum-rate optimization problem Arg-Init was the best performing method in terms of the average performance across different number of iterations. We fix the iterations to 100 and show the distribution of the performance of the methods across different problem instances in Figure 20. As we can see from the Figure 20 the distribution of Arg-Init is the most towards the left among all the distributions. We also provide the validation mean square error when learning h_{val} and h_{arg} . For Arg-Init (Val-Init) the MSE at the end of first epoch: 0.100 (0.0200) and at the end of last epoch: 0.0135 (0.0113).

8 Acknowledgement

We would like to acknowledge Karthikeyan Shanmugam for the valuable comments and feedback on the work.

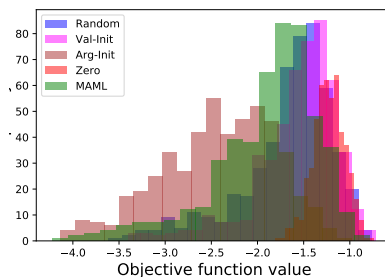


Figure 20: Sum rate optimization: Histogram comparing objective function values

References

- [Ackley, 2012] Ackley, D. (2012). *A connectionist machine for genetic hillclimbing*, volume 28. Springer Science & Business Media.
- [Andrychowicz et al., 2016] Andrychowicz, M., Denil, M., Gomez, S., Hoffman, M. W., Pfau, D., Schaul, T., Shillingford, B., and De Freitas, N. (2016). Learning to learn by gradient descent by gradient descent. In *Advances in neural information processing systems*, pages 3981–3989.
- [Antoniou et al., 2018] Antoniou, A., Edwards, H., and Storkey, A. (2018). How to train your maml. *arXiv preprint arXiv:1810.09502*.
- [Arthur and Vassilvitskii, 2007] Arthur, D. and Vassilvitskii, S. (2007). k-means++: The advantages of careful seeding. In *Proceedings of the eighteenth annual ACM-SIAM symposium on Discrete algorithms*, pages 1027–1035. Society for Industrial and Applied Mathematics.
- [Candes et al., 2015] Candes, E. J., Li, X., and Soltanolkotabi, M. (2015). Phase retrieval via wirtinger flow: Theory and algorithms. *IEEE Transactions on Information Theory*, 61(4):1985–2007.
- [Cheng et al., 2018] Cheng, M., Le, T., Chen, P.-Y., Yi, J., Zhang, H., and Hsieh, C.-J. (2018). Query-efficient hard-label black-box attack: An optimization-based approach. *arXiv preprint arXiv:1807.04457*.
- [Cheng et al., 2019] Cheng, M., Singh, S., Chen, P.-Y., Liu, S., and Hsieh, C.-J. (2019). Sign-opt: A query-efficient hard-label adversarial attack. *arXiv preprint arXiv:1909.10773*.
- [Chiang et al., 2007] Chiang, M., Tan, C. W., Palomar, D. P., O’neill, D., and Julian, D. (2007). Power control by geometric programming. *IEEE transactions on wireless communications*, 6(7):2640–2651.
- [Dauphin and Schoenholz, 2019] Dauphin, Y. N. and Schoenholz, S. (2019). Metainit: Initializing learning by learning to initialize. In *Advances in Neural Information Processing Systems*, pages 12624–12636.

- [Dhurandhar et al., 2018] Dhurandhar, A., Chen, P.-Y., Luss, R., Tu, C.-C., Ting, P., Shanmugam, K., and Das, P. (2018). Explanations based on the missing: Towards contrastive explanations with pertinent negatives. In *Advances in Neural Information Processing Systems*, pages 592–603.
- [Egozcue et al., 2009] Egozcue, M., Garcia, L. F., and Wong, W.-K. (2009). On some covariance inequalities for monotonic and non-monotonic functions. *Journal of Inequalities in Pure and Applied Mathematics*, 10(3):1–7.
- [Finn et al., 2017] Finn, C., Abbeel, P., and Levine, S. (2017). Model-agnostic meta-learning for fast adaptation of deep networks. In *Proceedings of the 34th International Conference on Machine Learning-Volume 70*, pages 1126–1135. JMLR. org.
- [Finn, 2018] Finn, C. B. (2018). *Learning to Learn with Gradients*. University of California, Berkeley.
- [Flennerhag et al., 2018] Flennerhag, S., Moreno, P. G., Lawrence, N. D., and Damianou, A. (2018). Transferring knowledge across learning processes. *arXiv preprint arXiv:1812.01054*.
- [Glorot and Bengio, 2010] Glorot, X. and Bengio, Y. (2010). Understanding the difficulty of training deep feedforward neural networks. In *Proceedings of the thirteenth international conference on artificial intelligence and statistics*, pages 249–256.
- [Goodfellow et al., 2014] Goodfellow, I. J., Shlens, J., and Szegedy, C. (2014). Explaining and harnessing adversarial examples. *arXiv preprint arXiv:1412.6572*.
- [Hu et al., 2009] Hu, X., Shonkwiler, R., and Spruill, M. C. (2009). Random restarts in global optimization.
- [Khalil et al., 2017] Khalil, E., Dai, H., Zhang, Y., Dilkina, B., and Song, L. (2017). Learning combinatorial optimization algorithms over graphs. In *Advances in Neural Information Processing Systems*, pages 6348–6358.
- [Koren et al., 2009] Koren, Y., Bell, R., and Volinsky, C. (2009). Matrix factorization techniques for recommender systems. *Computer*, 42(8):30–37.
- [Li and Malik, 2016] Li, K. and Malik, J. (2016). Learning to optimize. *arXiv preprint arXiv:1606.01885*.
- [Mairal et al., 2010] Mairal, J., Bach, F., Ponce, J., and Sapiro, G. (2010). Online learning for matrix factorization and sparse coding. *Journal of Machine Learning Research*, 11(Jan):19–60.
- [Martí et al., 2016] Martí, R., Lozano, J. A., Mendiburu, A., and Hernando, L. (2016). Multi-start methods. *Handbook of Heuristics*, pages 1–21.
- [Mishkin and Matas, 2015] Mishkin, D. and Matas, J. (2015). All you need is a good init. *arXiv preprint arXiv:1511.06422*.
- [Nocedal and Wright, 2006] Nocedal, J. and Wright, S. (2006). *Numerical optimization*. Springer Science & Business Media.
- [Pena et al., 1999] Pena, J. M., Lozano, J. A., and Larranaga, P. (1999). An empirical comparison of four initialization methods for the k-means algorithm. *Pattern recognition letters*, 20(10):1027–1040.

- [Ribeiro et al., 2016] Ribeiro, M. T., Singh, S., and Guestrin, C. (2016). " why should i trust you?" explaining the predictions of any classifier. In *Proceedings of the 22nd ACM SIGKDD international conference on knowledge discovery and data mining*, pages 1135–1144.
- [Schmidhuber, 1987] Schmidhuber, J. (1987). *Evolutionary principles in self-referential learning, or on learning how to learn: the meta-meta-... hook*. PhD thesis, Technische Universität München.
- [Schmidhuber, 1992] Schmidhuber, J. (1992). Learning to control fast-weight memories: An alternative to dynamic recurrent networks. *Neural Computation*, 4(1):131–139.
- [Strubell et al., 2019] Strubell, E., Ganesh, A., and McCallum, A. (2019). Energy and policy considerations for deep learning in nlp. *arXiv preprint arXiv:1906.02243*.
- [Thrun and Pratt, 2012] Thrun, S. and Pratt, L. (2012). *Learning to learn*. Springer Science & Business Media.
- [Tse and Viswanath, 2005] Tse, D. and Viswanath, P. (2005). *Fundamentals of wireless communication*. Cambridge university press.
- [Wichrowska et al., 2017] Wichrowska, O., Maheswaranathan, N., Hoffman, M. W., Colmenarejo, S. G., Denil, M., de Freitas, N., and Sohl-Dickstein, J. (2017). Learned optimizers that scale and generalize. In *Proceedings of the 34th International Conference on Machine Learning-Volume 70*, pages 3751–3760. JMLR. org.